Coatings **2015**, *5*, 142-171; doi:10.3390/coatings5020142

OPEN ACCESS

coatings

ISSN 2079-6412

www.mdpi.com/journal/coatings

Article

Correlation of Growth and Surface Properties of Poly(p-xylylenes) to Reaction Conditions

Andreas Reichel [1], Gerhard Franz [1,*] and Markus-Christian Amann [2]

[1] Department of Applied Sciences and Mechatronics, Munich University of Applied Sciences, Munich D-80335, Bavaria, Germany; E-Mail: andreas.reichel@wsi.tum.de

[2] Walter Schottky Institut, Technische Universität München, Am Coulombwall, Garching D-85748, Bavaria, Germany; E-Mail: amann@wsi.tum.de

* Author to whom correspondence should be addressed; E-Mail: gerhard.franz@hm.edu.

Academic Editor: Alessandro Lavacchi

Received: 2 March 2015 / Accepted: 30 April 2015 / Published: 8 May 2015

Abstract: Parylene, a non-critical, non-toxic layer material, which is not only a candidate for low-K dielectrics, but also well suited for long-term applications in the human body, has been deposited by (plasma-enhanced) chemical vapor deposition of the monomeric species. To that end, a specially-designed reactor exhibiting a cracker tube at its entrance, which serves as the upstream control, and a cooling trap in front of the downstream control has been applied. The process of polymerization has been traced and is explained by evaporating the dimeric species followed by dissociation in the cracker at elevated temperatures and, eventually, to the coating of the polymeric film in terms of thermodynamics. Alternatively, the process of dissociation has been accomplished applying a microwave plasma. In both cases, the monomerization is controlled by mass spectrometry. The window for surface polymerization could be clearly defined in terms of a factor of dilution by an inert gas for the chemical vapor deposition (CVD) case and in the case of plasma-enhanced chemical vapor deposition (PECVD), additionally by the power density. The characterization of the layer parameters has been carried out by several analytical tools: scanning electron microscopy and atomic force microscopy to determine the surface roughness and density and depth of voids in the film, which influence the layer capacitance and deteriorate the breakdown voltage, a bulk property. The main issue is the conduct against liquids between the two borders' hydrophilic and hydrophobic conduct, but also the super-hydrophobic character, which is the condition for the Lotus effect. The surface tension has been evaluated by contact angle measurements. Fourier-transform infrared spectroscopy has proven the conservation of all of the functional groups during polymerization.

Keywords: plasma-enhanced chemical vapor deposition; xylylene; parylene; morphology

PACS classifications: 05.70.-a, 07.20.Hy, 07.30.Kf, 0.75+h, 64.70.Fx

1. Introduction

Chemical vapor deposition is performed with excited gaseous species that chemically react on a cold surface to form a new compound. In most cases, two different gaseous precursors flow into the reactor, where the reaction occurs. For example, to deposit Si_3N_4, SiH_4 and NH_3 are activated, either thermally or by plasma, to form radicals that can react to form the desired coating. In most cases, a carrier gas, often hydrogen, which has a very large mean velocity, is used as a diluent to ensure stable, homogeneous reaction conditions; such conditions allow deposition to occur at very low deposition rates. Because the molecular speed of helium is similar to that of hydrogen, other research groups favor this ambient gas. The low density of the film-building reactants shifts the reaction path to surface polymerization (sometimes referred to as vapor deposition polymerization [1] or transport polymerization [2]), and this shift is reflected by shiny, transparent films. In contrast, if the reactants are present at high densities, parasitic volume polymerization leads to agglomeration in the vapor [3], which is incorporated into the layers and causes roughness and opacity [4,5]. Instead of reacting at the surface, at sufficiently high densities, collisions between activated molecules are very likely to happen, and volume polymerization competes effectively with surface polymerization. In contrast to the latter reaction, the volume polymerization is characterized by very small aggregates, which leads to grainy, opaque layers. The dimensions of these grains cover a range of three orders of magnitude, beginning on the lower nanoscale up to some micrometers in size. By the formation of these particles, the characteristics of the surface properties can be completely changed. In particular, the phenomenon of super-hydrophobic surfaces, as well as the commonly-known Lotus effect are suspected to be closely connected to the occurrence of nanoscale roughness [6–9].

For the polymerization of p-xylylene, with its commercial name parylene, which is widely used as a coating material for medical purposes [10,11], but also for isolating purposes with a pinhole-free film that is impermeable to water vapor and other gases, even at very low thicknesses [12,13], several reactions have to be investigated: "conventional" chemical vapor deposition happens by expanding at least one reactive gas in a vacuum reactor, which is either subjected to thermolysis or to a second gas, resulting in a chemical reaction. In contrast to these processes, parylene is mostly deposited by the Gorham process, which requires evaporation of a precursor, and temperatures between 130 and 150 °C are involved [14]. Second, the precursor has to be fragmented into reactive intermediates, which subsequently react in the third step to the polymeric chain.

Due to the inevitable evaporation during the heating ramp, which causes an irreproducible layer growth, very thin layers with reproducible accuracy are not accessible. This issue has been addressed either through the use of a heating system with a low thermal capacity of the heating system [15,16] or through the use of very small amounts of the precursor; see, e.g., [17–20]. Using this route, Stahl showed

that the deposition of 50 nm-thick films is possible. In this case, the pressure and the number density increase from zero to a certain saturation level after having reached the final evaporation temperature. When the amount of precursor is exhausted, the pressure and the number density decrease, which can drastically reduce the reaction rate (these surface reactions follow first-order kinetics). Mechanistically, pressure (and number density) start and end at zero, which causes an even stronger reduction of the reaction rate for a reaction of third order [21]. Preparatively, the number densities of the chain-building monomers and oxygen will become equal, and eventually, the latter will surpass the number density of the monomers. Consequently, the composition and properties of the interfaces will deviate from those of the bulk material. Thus, the vertical homogeneity deteriorates.

With our version of an improved Gorham process [14], we could deposit layers far below 1 µm in thickness very precisely [22]. To avoid the inevitable and irreproducible coating during the process of heating up to the final temperature, the reactor is maintained under an increased pressure of 40 Pa of argon gas, which inhibits the evaporation of diparylene. When the vaporizer has reached its target temperature, the pressure of the supporting gas is abruptly reduced to its target value, e.g., 5 Pa, and the coating process begins immediately at a constant deposition rate [23].

The evaporation step is followed by generating the reactive monomers *en route* as the dimers pass through a cracking tube driven at temperatures between 450 and 750 °C (*cf.*, Equation (1), [24–26]).

Only these monomers should be adsorbed by the "cold" surfaces to form polymeric chains in the next step; "cold" refers to temperatures less than 40 °C [19,27] or even less (below 30 °C, according to Odian [2], the so-called "ceiling" temperature [28,29]).

To deposit layers with vertical homogeneity, most industrial films are coated in a flow reactor, especially if plasmas are used. A flow reactor has been used in this work. Only with this reactor can plasma-supported reactions and thermally activated processes be compared. According to Yasuda, the first reaction is called activation [Equation (1.1)], and the second one is the passivation [Equation (1.2); Figure 1].

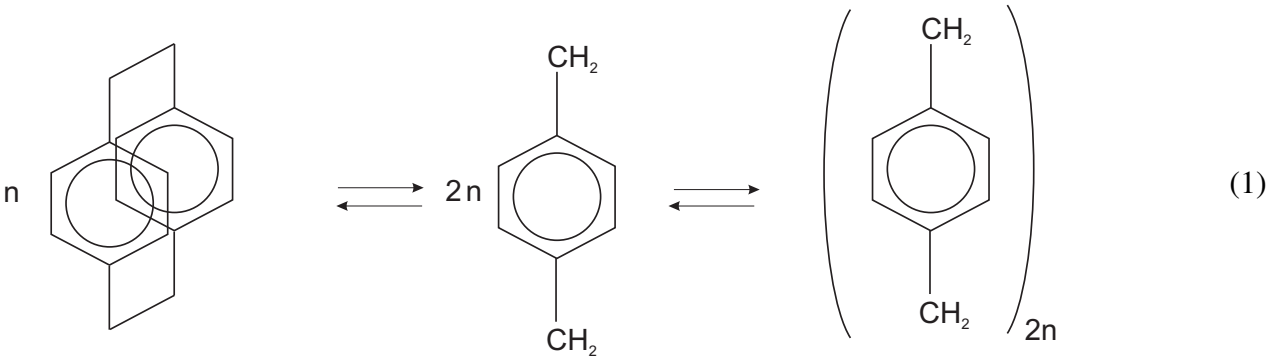

(1)

Figure 1. CVD process: (Left) The three-dimensional dimeric species (di-*p*-xylylene)—which contains two ethylene bridges in each *p*-position—is cracked (1: activation) to form the monomer (middle) (*p*-xylylene radical), which forms polymeric chains of *poly*-*p*-xylylene (2, right, passivation) [14]. This reaction can occur either in the gas (volume polymerization) or on the cold surface (surface polymerization).

The activation process is expected to roll from left to right with increasing temperature or with the optimum of ρ in plasmas.

Either thermal or plasma processes are required to ensure a certain density of chain-forming radicals. From the temperature-dependent equilibrium, measured by mass spectrometry, the energy of dissociation can be calculated to be 1.68 eV [23]. In a low-temperature plasma, activation, *i.e.*, fragmentation into radicals and ionization, happens by collisional impact between rapidly moving electrons and almost inert neutrals. Therefore, the extent of activation is measured by the ratio of the high frequency power P_{HF} to the flow of molecules F, which equals the ratio of energy input to the number densityof molecules:

$$\rho = \frac{P_{\mathrm{HF}}}{F} = \frac{E/t}{n/t} = \frac{E}{n}, \tag{2}$$

and n scales with partial pressure p_{i}. For low power input or high monomer flow, resp., the ratio remains relatively small; this is called the monomer-sufficient region. By raising the power or reducing the flow, the deposition rate can be increased easily. For large power input or low monomer flow, resp., further fragmentation reactions become superior to simple formation of chain-building radicals, resulting in a decline of the deposition rate. These two regimes are separated by a third section, the competition region. This region is distinguished by a constant deposition rate. Compared to radio frequency discharges where processes across the sheath have to be considered, the splitting into three regimes should be readily checked and confirmed in microwave discharges lacking high-voltage sheaths [4,18].

Hence, one of the main issues of this work is the correlation of several properties of the bulk and of the surface of the polymeric film with the activation process and the density of the reactive species, which has been the subject of various previous papers [23,30,31].

Here, we will concentrate on the properties of the polymeric coatings, which were deposited with various conditions of pressure (number density) and flow, which define an upper limit for smooth, translucent coatings, caused by the onset of volume polymerization. This border is also drawn by too high of a microwave power, which causes a destruction of the benzene ring structure, indicated and proven by IR spectroscopy. The term "plasma enhanced" is also discussed in terms of yield and a bulk property (layer thickness). However, the most prominent features are the surface morphology and the surface energy, which determine the behavior against water and nonpolar solvents, simply regarded as a hydrophobic or hydrophilic character, and, moreover, the super-hydrophobic conduct, as well, which is eventually treated.

2. Experimental Section

The apparatus consists of a microwave reactor (parallelepiped) of 91 L (40 × 40 × 57 cm^3) to which the evaporator is flanged via a gate (Plasma Parylene Systems, Rosenheim, Germany, Figure 2).

Pulsed microwave power (2.45 GHz) is generated within a commercially available R26 wave guide as a resonant cavity and is coupled to the reactor via a quartz window, which is arranged at the center of one side (4 in. in diameter). Several instruments for plasma diagnostics are connected to the reactor via KF 40 flanges: an energy-dispersive mass spectrometer for residual gas analysis and reaction control (Hiden HAL EPQ 300, Kochel am See, Germany), a Langmuir probe (Ruhr-Universität Bochum, Germany) and an optical emission spectrometer (OMA III, Princeton Applied Research, Oak Ridge, TN). They are described in detail elsewhere [32,33].

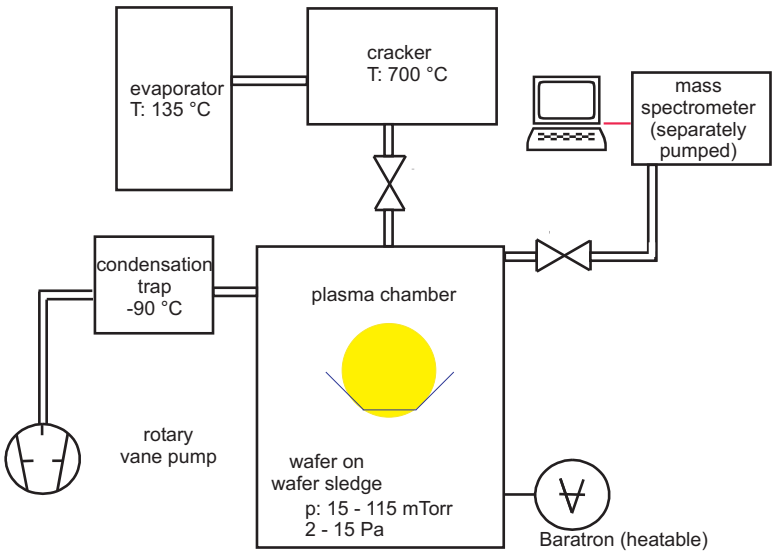

Figure 2. Sketch of the reactor with microwave source and microwave window and pumping system (condensation trap and rotary pump). Not shown are the diagnostic ports for optical emission spectroscopy and the Langmuir probes.

Between the pump and the exhaust, a cold trap is installed to catch abundant mono-parylene and non-reacted diparylene. The evaporator itself consists of a heating element and a relatively small container for the dimeric parylene. The system is extensively described in [23,30].

The coating process consists of evaporation of the dimer at a temperature between 110 and 130 °C for the N-derivate and 135 and 150°C for the C-derivate, which is subsequently decomposed into its monomeric species at temperatures beyond 620 °C (source: Plasma Parylene Systems, Rosenheim, Germany). Upon entering the deposition chamber, the deposition process takes place as polymerization. Since vapor pressure solely depends on temperature, by this procedure, the flow of the monomeric species is kept constant at approximately 9 sccm. This process can be supported by a microwave plasma, which is easily ignited, even at higher discharge pressures. Pumping by a rotary pump is supported by a condensation trap, which is operated at −90 °C. Base pressures are typically between 0.5 and 1 mTorr (0.2 Pa) and coating pressures (with or without a plasma) between 20 and 800 mTorr (3 and 100 Pa), controlled downstream by a valve (VAT, Switzerland). In some cases, the vapor is diluted by argon. For the unsubstituted cyclophane, at a 130 °C evaporation temperature and a 700 °C cracker temperature, the pressure in the reactor is 6 mTorr with pumping speed at maximum, measured with the heated Baratron B270 from MKS, without diluent gas. The vapor pressure of the C derivate is slightly higher, at a 110 °C evaporation temperature and a 700 °C cracker temperature; the pressure in the reactor is 7.5 mTorr. It is this value with which we start, the total pressure being reached by diluting with argon. Mass flow controllers of MKS (Munich, Germany) are used for O_2 and CF_4 for copolymerization; the parylene layers are attacked by an oxygen plasma generated in the microwave plasma system 100-E by Technics Plasma (Kirchheim, Bavaria, Germany).

The substrates to be coated are glass carriers for microscopy and three-dimensional medical tools, mostly capillaries and pipes, but also stents. Since, for diagnostic purposes, the addition of inert gas is required, we had to measure the deposition rate as a function of the fluxes of monomeric species

and inert gas (argon) [30,32]. The deposited layers are analyzed by inspection with SEM, AFM with a micro-cantilever of OMCL-RC Olympus as a scanning tip and impedance analysis (low frequency and high frequency), applying electrochemical impedance spectroscopy (4192 A Impedance Analyzer of Hewlett-Packard), and by determination of the contact angle with two different liquids (H_2O as a prototype for a polar solvent and CH_2I_2 as a prototype for a highly polarizable, but almost nonpolar solvent). Here, the so-called pendant-drop method is applied: The contact angle of a drop lying atop the substrate is measured. Applying the procedure according to Owens and Wendt, the total surface energy and their polar and dispersive fractions can be evaluated [34]. To check the integrity of the molecular structure during deposition and to look for new functional groups, several films have been analyzed applying Fourier-transformed IR spectroscopy (Bruker, Inc., Billerica, MA, USA).

3. Results and Discussion

3.1. Introduction

The rate-limiting step of the polymerization is the cleavage of the bridge between the two methylene groups (Figure 1), which can be performed either thermally, or by plasma activation, or by a combination of both methods. In all cases, the cleavage is supposed to be the main reaction, but it is definitely not the only track for how the molecules can be attacked. Both methods compared, the plasma is the more sensitive environment, which is proven by numerous inorganic reactions that can be generated, but in a plasma (interhalogenic compounds), itdoes not exhibit a thermal activation; therefore, no activation energy can be determined.

3.2. Dissociation

3.2.1. Thermal Activation

The cleavage can be investigated by mass spectrometry (Figure 3). For the monomer *p*-xylylene, the most prominent peak can be found at 104 amu (monomeric CH_2–C_6H_4–CH_2, intensity: 1.0), followed by the pattern sequence 91 (tropylium cation, intensity: 0.04), 78, 77 (78: benzene, intensity: 0.4, 77: benzene−hydrogen, intensity: 0.29) and 52 (C_4H_4, fragment of benzene, intensity: 0.29). Starting at about 400 °C, the peak at 104 rises continuously up to the highest temperature of 700 °C and is used to determine the equilibrium between the dimeric and monomeric species. For the mono-chlorine-substituted *p*-xylylene, the most prominent peak is found at 103 amu (the M^+ peak of the monomer with Cl abstracted: CH_2–C_6H_3–CH_2). From an Arrhenius plot, the energy of dissociation yields 1.68 eV for this species [23] (Figure 4). In fact, the dissociation energy is the activation energy for this dimerization. The resulting fragments are identical to the end products of the reaction. Two monomers are generated from one dimeric molecule. A series of fragments is created for the chlorine derivates.

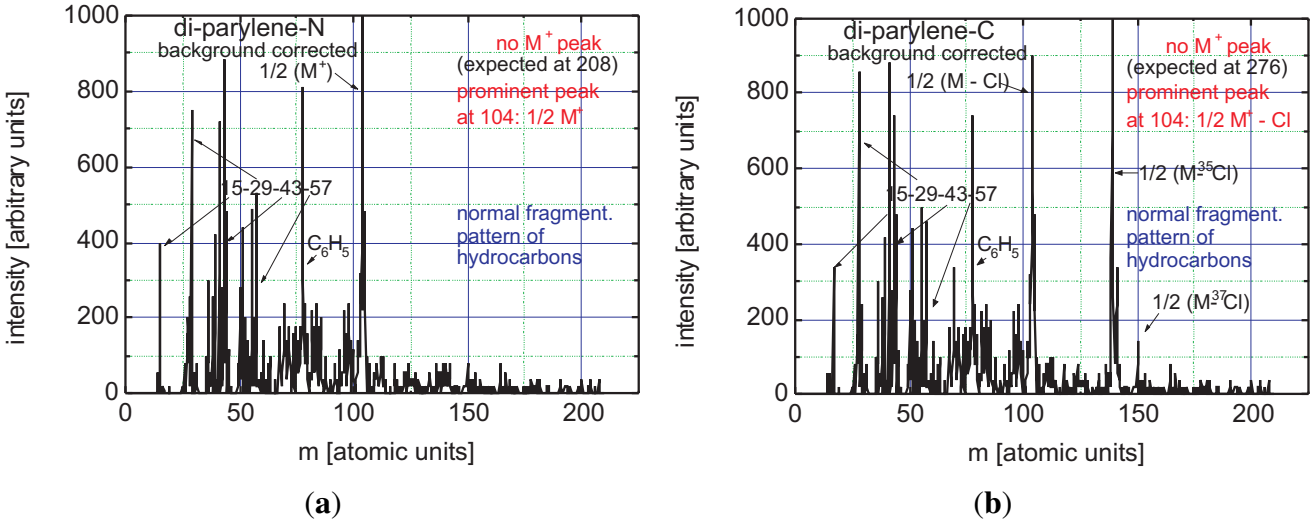

Figure 3. CVD of the thermally-cleaved dimeric precursor N (**a**) and C (**b**) and its control by mass spectrometry (the $^1/_2$ M^+ peak is set to 1000).

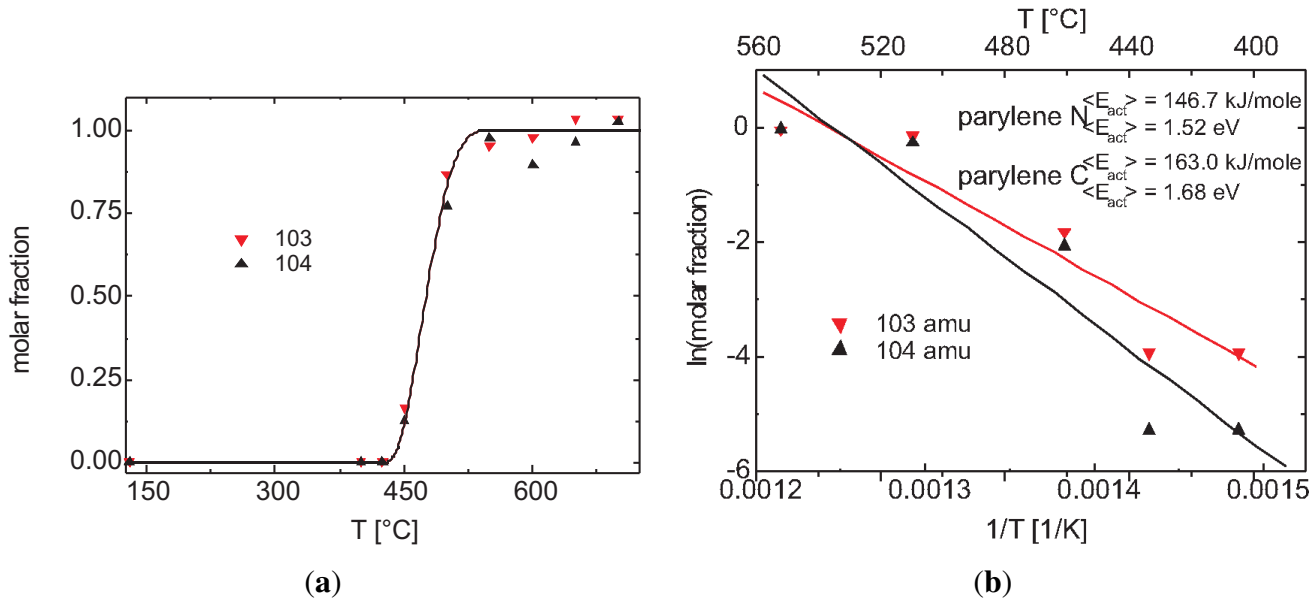

Figure 4. (**a**) Peaks (Gaussian bell curves) at 103 and 104 amu, resp., *vs.* the temperature of the cracker. (**b**) The heat of dissociation can be evaluated to approximately 1.52 eV for the unsubstituted paracyclophane and to approximately 1.68 eV for the mono-chlorine substituted species.

To avoid deposition of the vaporous dimer, the pipe between the cracker and the entrance must be heated to temperatures greater than 150 °C. If the temperature within this tube does not reach this level before the cracker was heated to 450 °C, then this equilibrium could not be determined accurately. To rule out this possibility, we monitored the residual mass spectrum throughout the heating process. Most prominent is the complementary behavior of masses 104 and 32 (Figure 5). The increase at 104 amu ($M^+/2$) is obviously accompanied by a steep decrease at 32 amu: the oxygen molecules are trapped, and the monomeric species must be the trap.

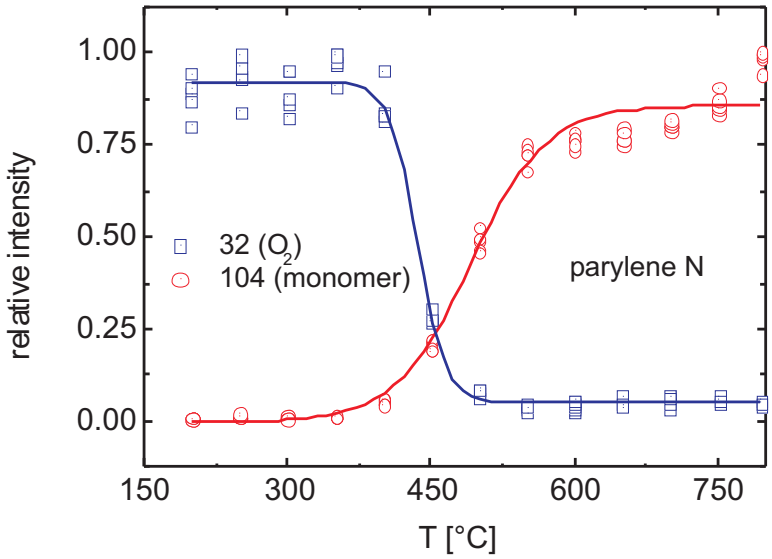

Figure 5. By comparison of the masses for oxygen (32 amu) and the monomeric species of the unsubstituted monomer (104 amu), it is proven that oxygen is trapped by the monomer. This can occur only at a cracker temperature of at least 450 °C (sigmoid fit).

3.2.2. Plasma Activation

From Figures 3 and 4, it is evident that for effective thermal cleavage, a certain threshold temperature is required. This does not hold true for plasma activation, where the monomers are excited to higher electronic levels from which further reactions can readily occur (formation of radicals and ions). As has been outlined by Yasuda, the yield of the polymerization, *i.e.*, the thickness and density of the deposited layer as the simplest parameter, but above all, the purity, is a trade-off of the intended reaction paths (*i.e.*, the dissociation) and unintended reactions, here further destruction of the monomer at higher power input (*cf.*, Figure 6 [4]).

The maximum of the parabola, which describes the deposition rate, is supposed to be the onset of passivation [4], which is caused by the rising fragmentation of chain-building monomers (100 W corresponds to approximately 1.1 W/L). With this optimized power input, the growth rates are compared, made up of layers, which were piled up with the same amount of dimeric parylene (Figure 7).

3.2.3. Discussion

Efficiency for Thermal Cleavage

At typical conditions, in our reactor with a volume of 91 L ($40 \times 40 \times 51$ cm^3; $T_{\mathrm{evap}} = 130$ °C), we find a flow into the reactor of 9.3 sccm after evaporation and 18.6 sccm after complete dissociation (*i.e.*, 2.5×10^{20} molecules/min or 1.51×10^{22} dimeric molecules/h and 3.02×10^{22} monomers/h), which is a total of 50 m moles or 5.22 g. The area of the reactor is ($V = 40 \times 40 \times 51$ cm^3) 12,320 cm^2. If all monomeric molecules were stuck after their first surface hit, that would cause a current density of

$j = 6.8 \times 10^{14}$ monomers/cm^2, which would result in a layer growth of 3.84 µm (density of parylene N: 1.1 g/cm^3): no losses, no cooling trap required.

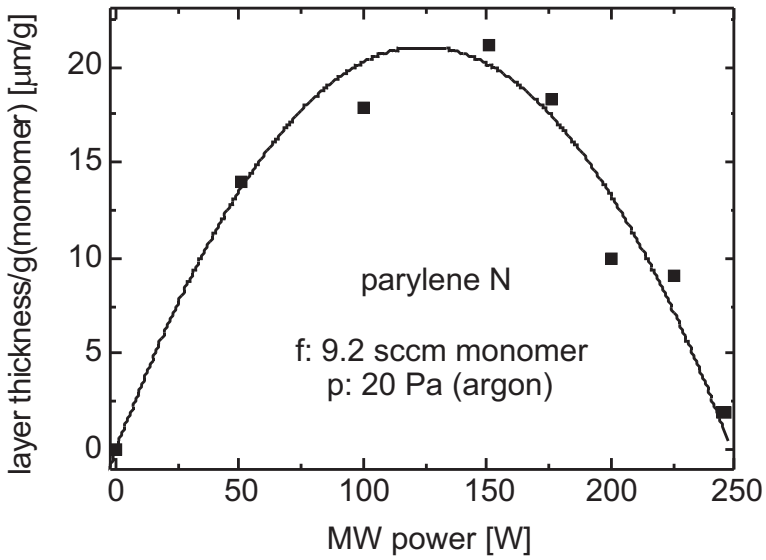

Figure 6. Regimes of power deficit and abundance of power are separated by optimum power input [4].

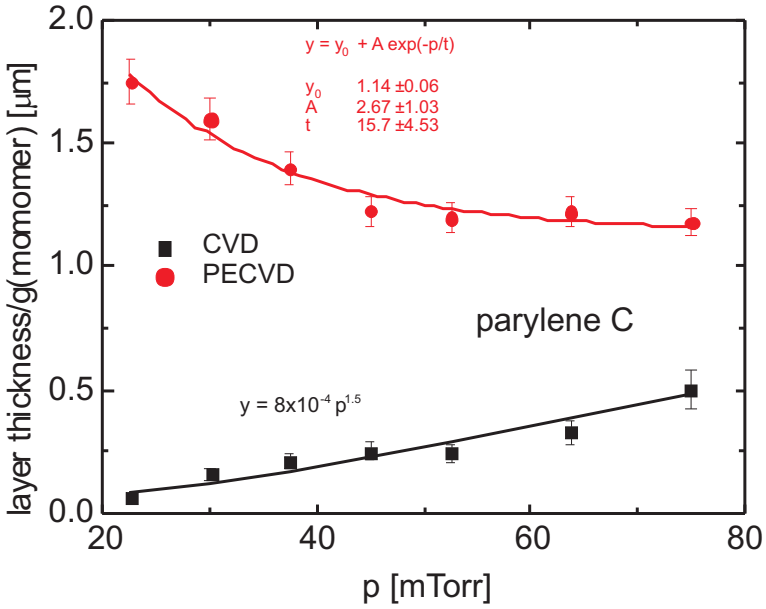

Figure 7. Comparison of the specific thickness of layers deposited (referring to the mass of the dimer) as a function of pressure for CVD and PECVD (MW power 125 W). By plasma application, the amount of reactive species is enhanced. However, due to the lower electron density with increasing pressure, the rate of layer formation decays exponentially.

At a pumping power of 3 L/s, the flow of 18.6 sccm of argon would cause a rise in pressure to 10.5 Pa, which equals a number density of $n = 5.75 \times 10^{19}$ molecules in 91 L or 6.4×10^{14} cm^3.

According to kinetic gas theory, we would expect a current density to either wall of 4.24×10^{18} cm^2/s, provided the hot monomers are thermalized to 300 K. Are they thermalized? A rough estimation for two conditions, either pure monomer or monomers diluted by argon, is:

- entering velocity (T = 1000 K): 480 m/s, $\sigma_{C_6H_6}$ = 88 Å^2, p = 10 Pa (6.4 × 10^{14} cm^3): λ = 1.25 mm;
- entering velocity (T = 1000 K): 480 m/s, σ_{Ar} = 36 Å^2, p = 40 Pa (25.6 × 10^{14} cm^3): λ = 0.8 mm.

As the reactor dimensions d are some tens of cm, in both cases, the ratio of reactor dimension $d \div \lambda$ is in the order of some tens: the vapor is completely thermalized.

From these estimations, we see that more than 6000 collisions with the surface are required to cause a yield of 100% (3.76 µm). Therefore, the process of deposition is reaction-rate limited and definitely not limited by diffusion, in good agreement with the modeling work of Rogojevic *et al.* [35]. In fact, it is a yield of 78%. To put it another way, more than $^1/_5$ of the monomer will get lost in the cooling trap.

Considering this equilibrium, we can compare the effective pressure rise with increasing temperature with the linear pressure rise without dissociation and with dissociation, but without polymerization (Figure 8). Since we work in the Knudsen regime between molecular and viscous flow, we calibrated the flow pressure relation by argon. From this, we calculated a pumping speed of S = 3.0 L/s. From this data and the reactor volume, we calculate a residence time of exactly 30 s. Complete dissociation and perfect pumping without deposition would cause a throughput of 0.2351 Torr/s and a rise in pressure to 79 mTorr in argon. Due to polymer formation, the pressure rise in mono-parylene is only 6 mTorr, and the pumping speed has apparently increased to S = 39.2 L/s, by more than a factor of 10.

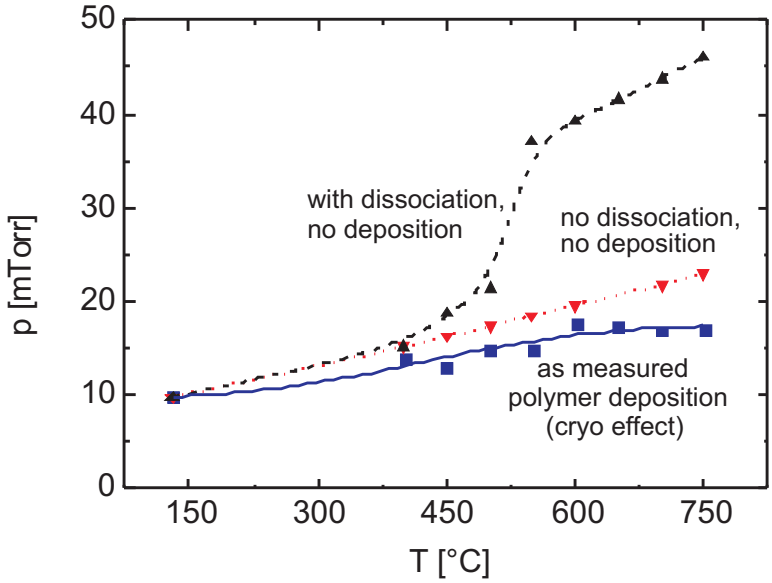

Figure 8. Comparison of the actual pressure with two scenarios: linear pressure rise due to the ideal gas law and increased pressure rise beyond 375 °C (onset of the dissociation).

Plasma Cleavage

Following the approach of Yasuda and Hirotsu, we rather refer to the thickness per mass of dimer as a function of pressure for CVD and PECVD than to the deposition rate. Since we only refer to one

sort of starting molecule, the dimer, it is not necessary to scale it with the molecular weight [18]. By plasma application, the concentration of layer-composing species is enhanced. However, due to the lower electron density with increasing pressure and the decreasing electron temperature, the rate of layer formation decays exponentially [36], but remains above the CVD branch (Figure 7; further discussion in Section 3.3).

Surface Polymerization *vs*. Volume Polymerization

From epitaxial growth, it is well known that the quality of the layers strongly depends on the degree of dilution of the vapor. Since one of the main issues of our research is the dependence of the porosity of very thin layers as a function of growth conditions and absolute thickness [31], we are interested in slowly-grown, but high-quality layers, which are the result of a surface polymerization, the volume polymerization forced back by diluting the vapor with argon.

The first step to initiate the polymerization consists of the formation of the dimeric radical out of three monomers, which yields an order of the reaction n of $\frac{3}{2}$ (roughly speaking: three for three molecules to be involved in the time-limiting step, $\frac{1}{2}$ for the symmetric cleavage of the precursor) [21,37]. As has been pointed out by Olson, this dimerization is energetically orientated uphill [38]. To form an oligomer, other monomers must dock to this twin radical to form a molecule that eventuallyexceeds the thermodynamic stability of its reactants. To form such an oligomer in the vapor, a high vapor density is required, which defines an upper limit of the operating pressure due to the onset of parasitic snow formation (approximately 100 mTorr) [21]. At the surface, however, this initial reaction has already occurred, and the propagation to longer chains simply happens as a reaction of first order; chain growth scales with an exponential decrease in vapor density. By diluting the chain-building vapor with argon, the growth rate is reduced (Figure 9). By variation of the evaporation temperature, which enhances the number density of the film-building species following the Clausius–Clapeyron equation, and all other parameters being kept constant, we fitted the pressure dependence of the deposition rate by an exponential law for a reaction of first order with almost the same exponent; a criterion for a reaction of first order. From the morphological point of view, formation of snow is definitely suppressed, leading to high-quality films at the expense of a lower growth rate (Figure 10).

3.3. Bulk Properties

We see from this discussion that almost all of the monomers are caught within the reactor. Figure 7 shows an enhancement factor for layer thickness of a factor of 1.5 or higher. This can be caused only by a lower density. Because parylene is one of the most promising candidates for low-K dielectrics, the properties that are the subject of current research are the frequency behavior of the impedance, the relative permittivity or the dielectric constant and the index of refraction.

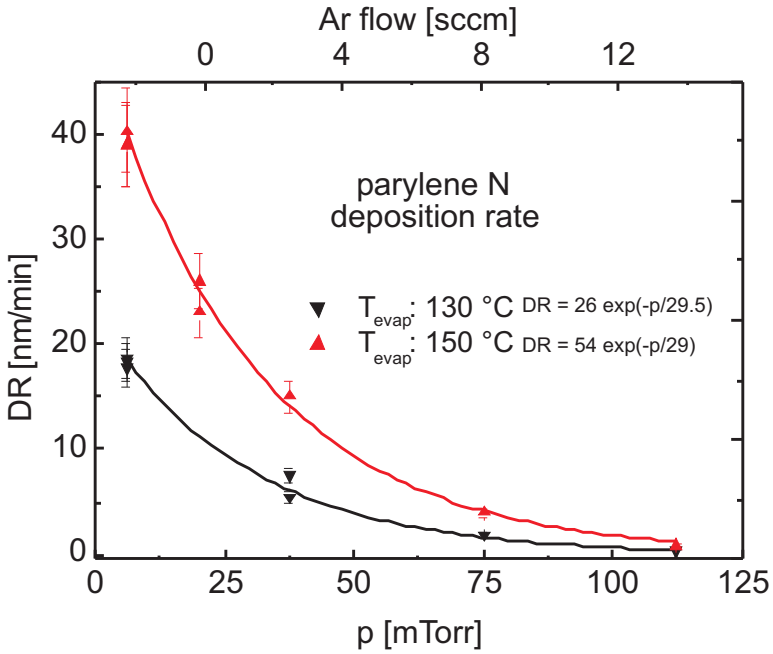

Figure 9. Deposition rate of parylene N. By diluting the vapor with argon, the reaction is forced to surface polymerization (reaction of first order).

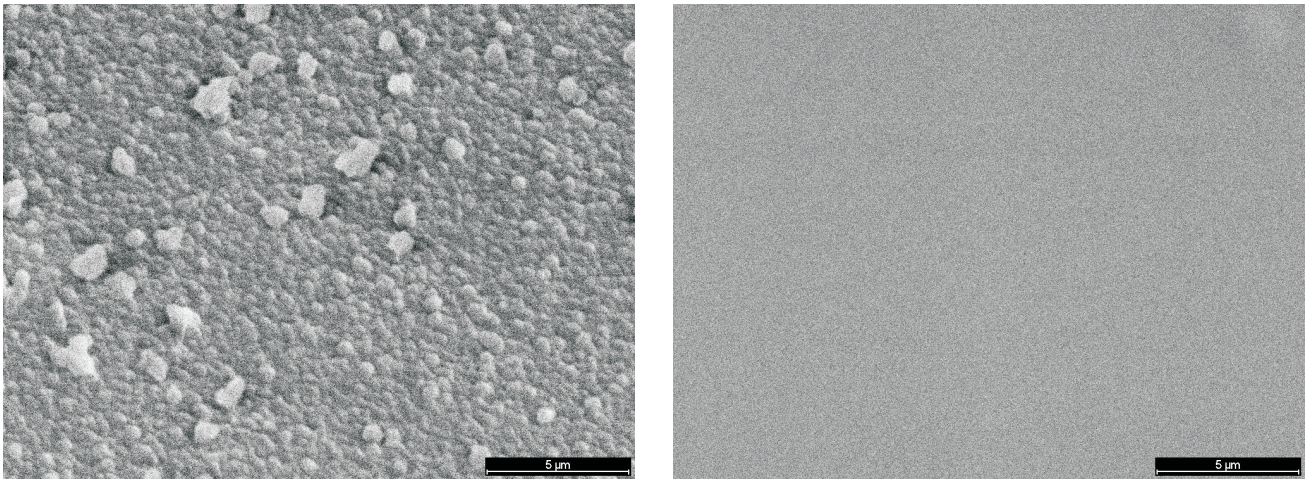

(**a**) (**b**)

Figure 10. Parylene N, deposited in a pure atmosphere of *p*-xylylene [(**a**) total pressure: 6 mTorr] and diluted by argon [(**b**) total pressure: 50 mTorr]. At constant partial pressure of the monomer, the volume polymerization at low pressure is effectively forced back.

In Figure 11, the areal capacitance of layers of CVD parylene C is depicted as a function of thickness, measured with electrochemical impedance spectroscopy. For layers beyond 200 nm in thickness, the relative permittivity levels off to values close to three (literature value at 1 MHz: 2.95 [38]). The steep increase for the permittivity below 200 nm is caused by the rising porosity, whereas the values for layers thicker than 400 nm match perfectly with the impedance shown in Figure 12, where the frequency dependence of the capacitance is shown in the low-frequency regime up to 100 kHz. The value starts at an almost constant bottom level at 3.1 to rise to lower frequency values (literature value at

1 kHz: 3.10 [38]). Following Maxwell's relation for the index of refraction, the literature value of linebreak $n = 1.64$ cannot be reached; the values scatter around [38], whereas the values for the PECVD-generated films are lower according to tendency, which is inferred by the lower density of the PECVD grown film (Figure 13). This shape is complementary to the recording of the dielectric function, performed by Mitu *et al.* [39], who have found that in an RF-driven discharge, medium ratios for power input and flow yield the lowermost values for ε: at low values, the dimeric species remains almost unaffected; at large values, the ring structure is destroyed (*cf.*, Section 3.4).

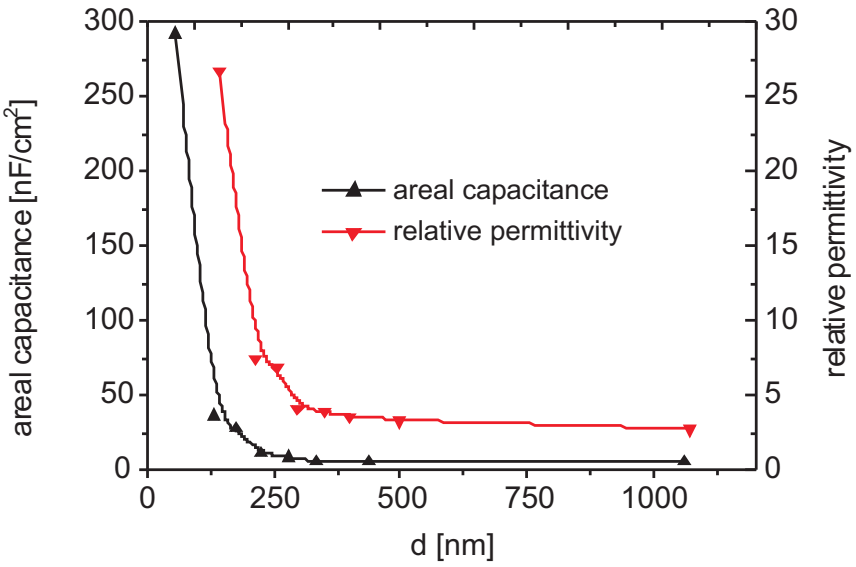

Figure 11. Areal capacitance of CVD layers of parylene C and resulting permittivity as a function of thickness as measured with electrochemical impedance spectroscopy at 1 MHz.

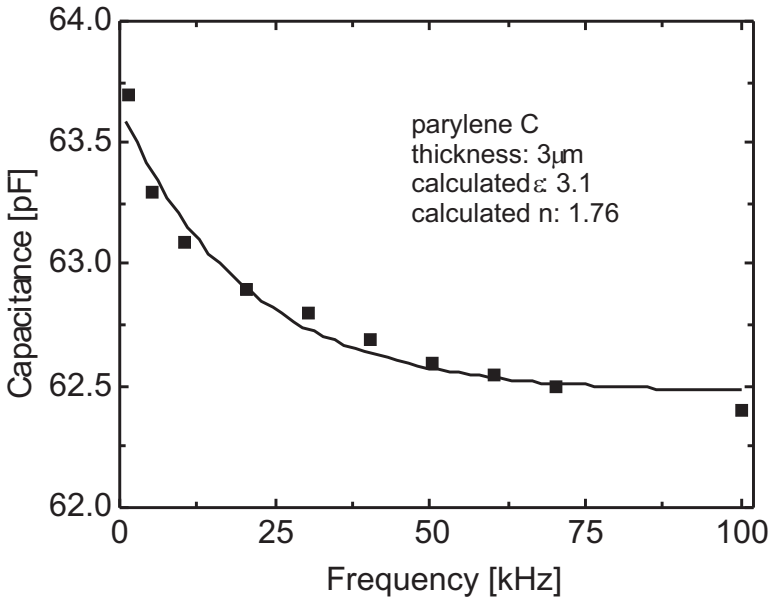

Figure 12. Low-frequency capacitance of CVD layers of parylene C and resulting permittivity as a function of frequency.

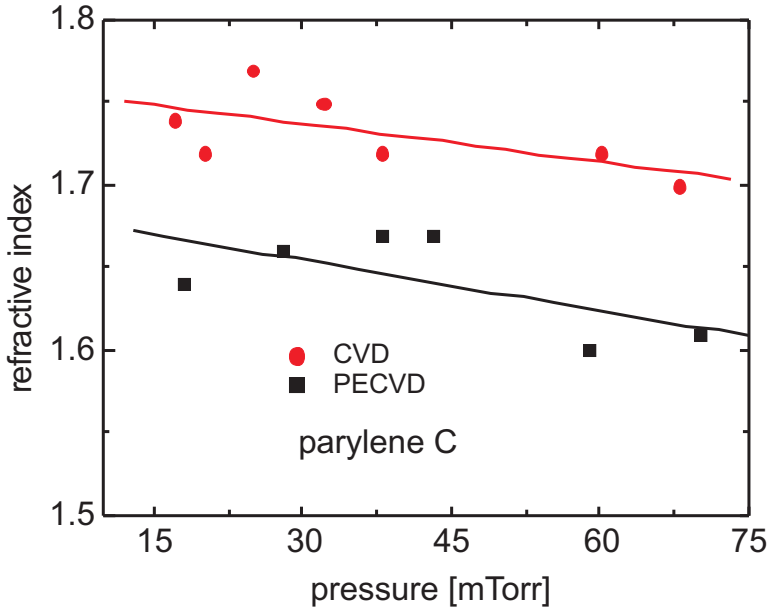

Figure 13. Comparison of the refractive index for films of parylene C, deposited either by CVD or PECVD.

3.4. Spectral Identification

In a plasma, the deposited layers are not only subject to attacks of fast ions and electrons, but also to energetic UV radiation. In particular, it is well known that oxygen-containing polymers, like PMMA, are prone to rapid degradation. Other polymers remain more stable, especially those which contain a benzene ring, for example polystyrenes.

For identifying functional groups, we applied Fourier-transformed infrared spectroscopy of layers that were up to 1 µm in thickness and were deposited on fragments of a GaAswafer. Hence, all of the spectra are difference spectra.

Because of the non-polarity of all of the bonds, no intense lines can be expected. The only question that can be answered in a positive sense is whether the ring structure has still "survived" or not. To answer this question, three windows are important: the uppermost region at 3000 cm^{-1} for the valence vibration of the C-H bond (ν_{CH}), the medium region at 1600 cm^{-1} for the valence vibration of the C–C bond (ν_{CC}) and the lowermost region at 800 cm^{-1} for the deformation vibration of the C–C bond (δ_{CC}).

From these, the medium region does exhibit the most intense lines, and a positive proof can be drawn from the occurrence of the vibrations in the region between 1500 and 1600 cm^{-1} (Figure 14). Both of the layers show the deformation vibrations and ring vibrations (δ_{CH_2}: 1404, 1452 cm^{-1}, ν_{ring}: 1495, 1609 cm^{-1}). The line at 1558 cm^{-1} is due to Cl-substitution and, consequently, does not occur in the N-derivate.

The infrared transmission spectra of parylene C and parylene N are consistent with earlier works by Streitwieser and Ward, who pointed out that the addition of an inert gas, like Ar, to a vapor of toluene, a derivate of benzene, leads to the microwave-induced generation of several several compounds in which the ring structure was still conserved [40]. However, they contradict the results of Olson, who investigated films deposited by conventional CVD [38], and also with those results that were obtained by radio-frequency generated plasma polymerization of styrene, by which the ring structure was

destroyed [17]. The reason for this different behavior, which is reflected in surface properties (see below), is still an area of current research. Perhaps the molecules are subjected to the higher electromagnetic field and the static DC field across the hot electrode in RF discharges and are consequently destroyed more readily than by microwave excitation [41,42].

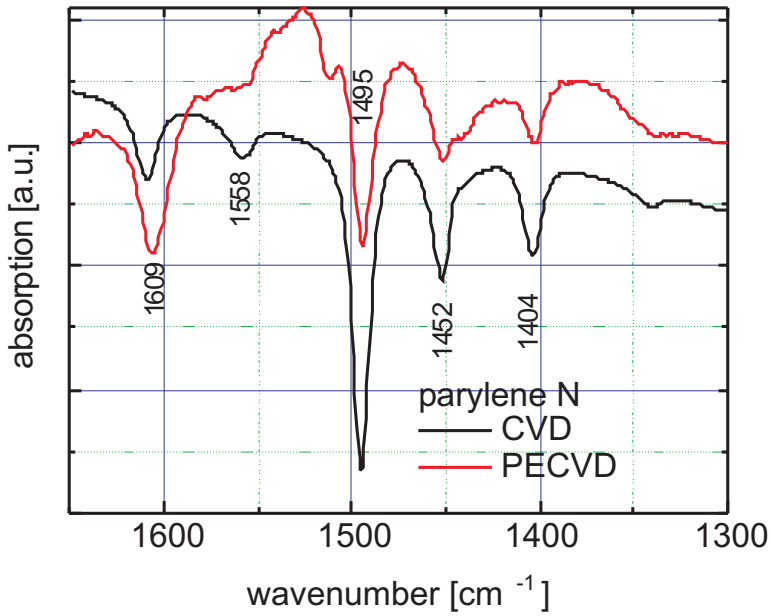

Figure 14. Detail of the IR spectrum of PECVD parylene N and CVD parylene N.

3.5. Surface Properties

We investigated tribological properties: contact angle and the resulting surface energy, which is completed by SEM micrographs and AFM graphs of the surface. As outlined in Section 2, the contact angle has been measured using two different fluids [34]. To decide whether the application of a microwave plasma alone can open a window to new surface properties, which are distinguished from the thermally-activated process, the N-derivate was evaporated without any cracking procedure. The C-derivate, however, was exposed to both sources, the microwaves and temperature. Here are shown:

- parylene N: CVD and pure PECVD;
- parylene C: CVD and thermally-assisted PECVD;
- parylene C: CVD, copolymerized with CF_4.

Since the resulting properties for the two parylenes C and N (pure and with the dopant CF_4) are very different, they are presented separately.

3.5.1. Parylene N

Contact Angle and Surface Energy

The behavior for the non-substituted species (CVD) shows the typical behavior that is expected for aromatic polymers: lipophilic character (very low angles against CH_2I_2), which is combined with

extremely hydrophobic properties (90°); Figure 15. The contact angle of the films does not exhibit any dependence on pressure, but the support of microwaves assists in enlarging the hydrophilic character, leaving the lipophilic conduct almost unchanged.

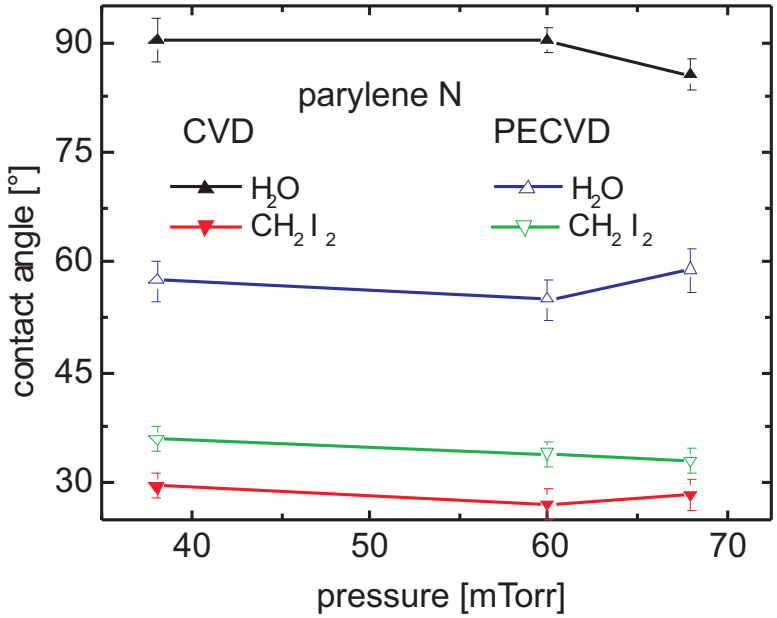

Figure 15. Different shape of the contact angle for parylene N (CVD and PECVD). The CVD coating is significantly more hydrophobic than the PECVD one, but also more lipophilic.

Extending the experiment of determination, the yield for both of the processes CVD and PECVD (Figure 7) by enhancing the microwave power with a topmost level of 250 W, the growth rate decreases after having reached a broad summit at approximately 125 W (Figure 6). At 250 W, the growth is almost zero, which is accompanied by a linear decrease of the contact angles against water, *i.e.*, the surface becomes more hydrophilic in character (Figure 16).

Although AFM measurements reveal a medium-rough surface, the wettability reaches low values (here, 45° at a microwave power input $P_{\mathrm{MW}} \approx 225$ W, p = 22 mTorr (3 Pa); according to Cassie's equation, roughening reduces the hydrophilic character [43]); Figure 17.

This behavior is inferred by the excitation by a plasma, but it is not caused by the main component, but by the residual gas O_2, which will become obvious by the following discussion concerning the surface behavior.

3.5.2. Parylene C

Contact Angle

Coatings of parylene (CVD) are significantly more hydrophobic than deposits coated by PECVD, whereas the differences concerning the lipophilic character are not very distinct. Therefore, only for the CVD deposit is the contact angle adjustable by the parameters gas flow and pressure (Figure 18). At the highest pressures, the contact angles are at their limits: at the lower level (lipophilic behavior), the angle is extremely flat, whereas at the upper limit (hydrophobic behavior), the water droplet is compressed

by its own weight. The values at 18 and 38 mTorr were obtained in a two-fold way: either solely with the evaporation of the dimeric species (flow: 4.6 sccm) or with some argon added (flow: 5 sccm) and compensating higher pumping speed; but we obtained nearly the same value for the surface tension.

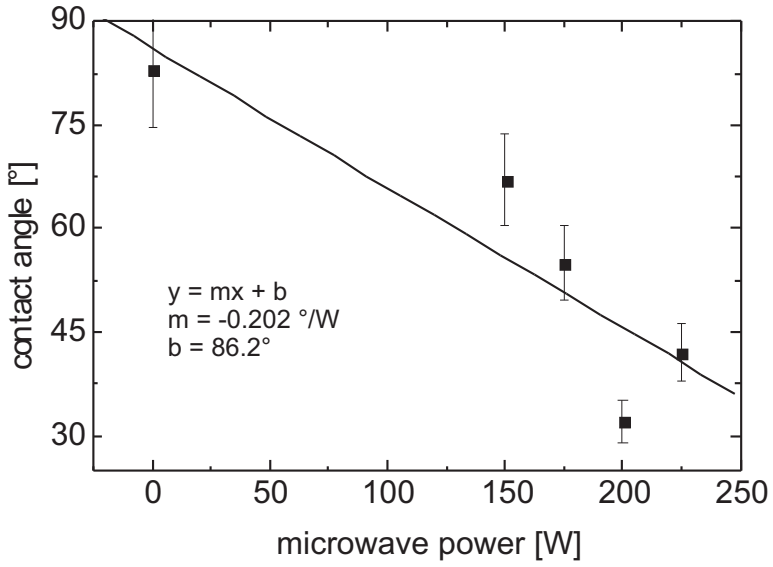

Figure 16. Contact angle of films of parylene N against water. With rising microwave power, the films become increasingly hydrophilic in character.

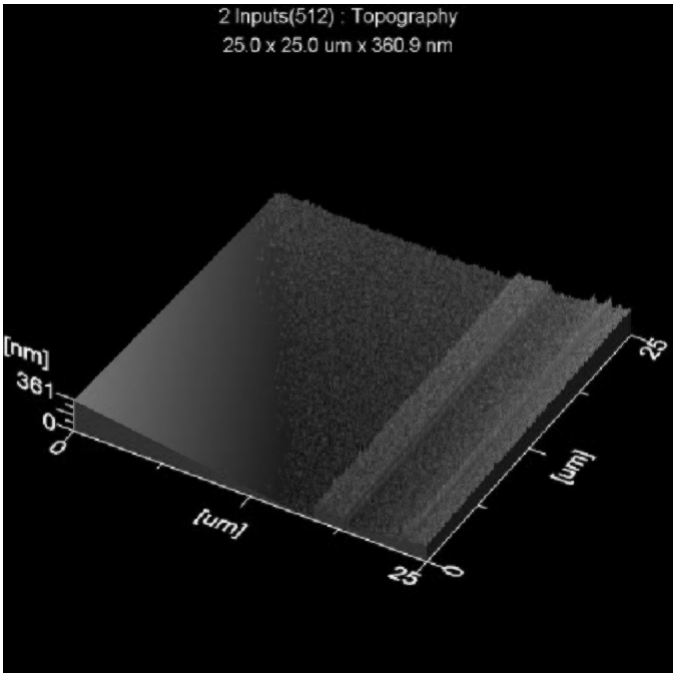

Figure 17. AFM micrograph of a CVD film of parylene N, deposited at 22 mTorr (3 Pa), exhibiting a medium-rough surface.

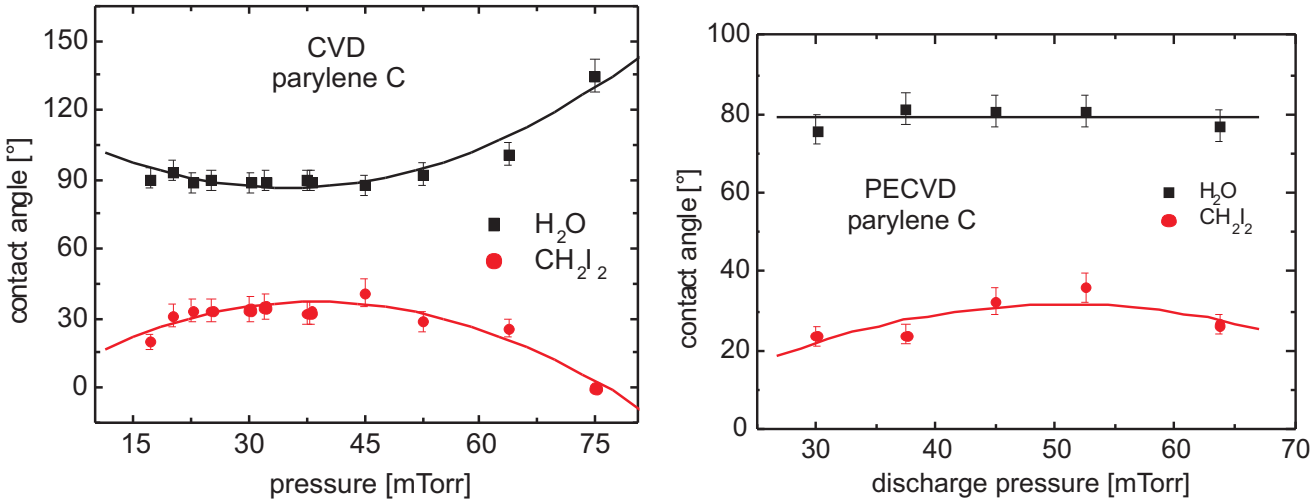

(**a**) (**b**)

Figure 18. Different shape of the contact angle for (**a**) CVD polyparylene and (**b**) PECVD polyparylene C. CVD polyparylene is significantly more hydrophobic than PECVD polyparylene.

Surface Tension

The surface energy of the CVD polymers can be varied across a large range: with growing pressure, the surface tension will increase by almost 100% for the plain CVD (Figure 19).This does not hold true for the plasma-enhanced variation. In contrast to this method, the surface energy remains remarkably constant over the covered pressure range. The split into the polar and dispersive fraction does show some movement at higher discharge pressures, but they are contradictory and cancel each other. Rising contact angles against CH_2I_2 lead to falling surface energies.

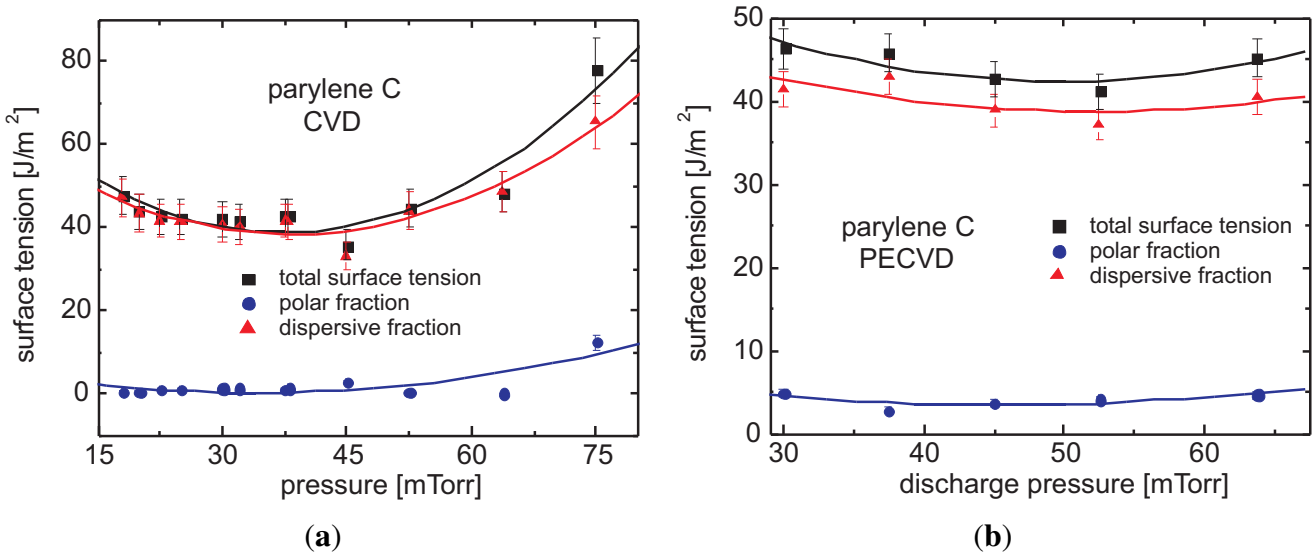

(**a**) (**b**)

Figure 19. Different shape of the surface tension of (**a**) CVD and (**b**) PECVD polyparylene C. The microwave power was between 100 and 150 W (1.1 W/L and 1.6 W/L).

3.6. Surface Behavior

There are at least two main reasons that can influence the conduct of surfaces against water, a chemically-based cause and a physically-based one.

3.6.1. Incorporation of Hydrophilic Groups

For an end vacuum of 0.5 mTorr ($^1/_{10}$ Pa), the number density of residual oxygen is 1.7×10^{13} cm^3. For a "normal" process, the evaporation rate is 4.5 sccm in our large reactor (volume: 90 L); after the thermal cleavage, it doubles its value to 9 sccm. Argon is added to dilute the vapor. In the equimolar case, the pumping speed is approximately constant at 2.4 L/s. Hence, the number density of the monomers is 3.7×10^{15} cm^3, which results in a ratio of monomers to oxygen molecules of only 220. For comparison, if Al is being sputtered reactively in an ambient gas doped with O_2 at a typical deposition rate of 1 µm/min, a partial pressure of just 0.5 mPa (5×10^{-6} Torr) is sufficient for complete oxidation (56 atomic percent of oxygen). Using the equation connecting current density to drift velocity $j = \rho \times v$ to estimate the density of the Al atoms located between the electrodes, it is evident that termination will most likely occur by oxygen capture. In the case that E_{kin} equals 4 eV, the initial velocity of the Al atoms is approximately $1/\sqrt{(3/4)28} = 33 \times 10^5$ cm/s. If the energy is reduced to 1 eV when the atom hits the surface, the velocity still remains at 2×10^5 cm/s. With an area of 8 Å^2 required for one Al atom, a flux of 8×10^{16} atoms/cm^2/s results, which translates to a density of 11×10^{11} atoms/cm^3. The partial pressure of oxygen is lower by only one order of magnitude (1.6×10^{11} atoms/cm^3).

This termination reaction undoubtedly causes a reduction in chain length and a switch to hydrophilicity, because oxygen will form CH(OH)- and C=O-groups.

In every case, the residual gas vacuum is of the order of $^1/_2$ Pa (4 mTorr), which is the lower vacuum limit for conventional rotary vane pumps. This residual vacuum means that the residual gas pressure of oxygen is on the order of 1 mTorr, and the O_2 diradical easily terminates the polymeric reaction via Equation (3), or through other termination reactions. This behavior may influence the degree of polymerization (chain length) and eventually influence the film density, thus resulting in inhomogeneous layers.

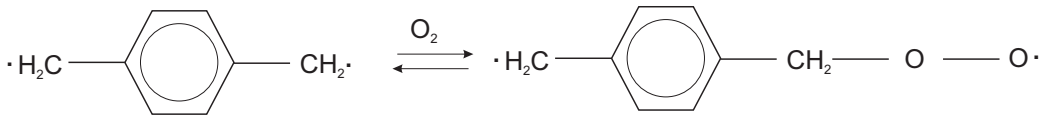

(3)

3.6.2. Surface Roughness

From the equations of Wenzel [44], it is obvious that the conduct of a surface against polar and nonpolar solvents (*i.e.*, hydrophilicity and hydrophobicity) is amplified by its roughness. For very rough surfaces, the application of the Cassie equation reveals that even hydrophilic surfaces can be transformed to hydrophobic surfaces [43].

We addressed this field by comparing the surface roughness as a function of total pressure for the two excitation methods, thermal and plasma dissociation. At low pressure (22 mTorr), the micrographs

of parylene C exhibit some details of a very smooth pin-hole free surface, irrespective of whether the deposition method has been simple CVD or PECVD (Figure 20).

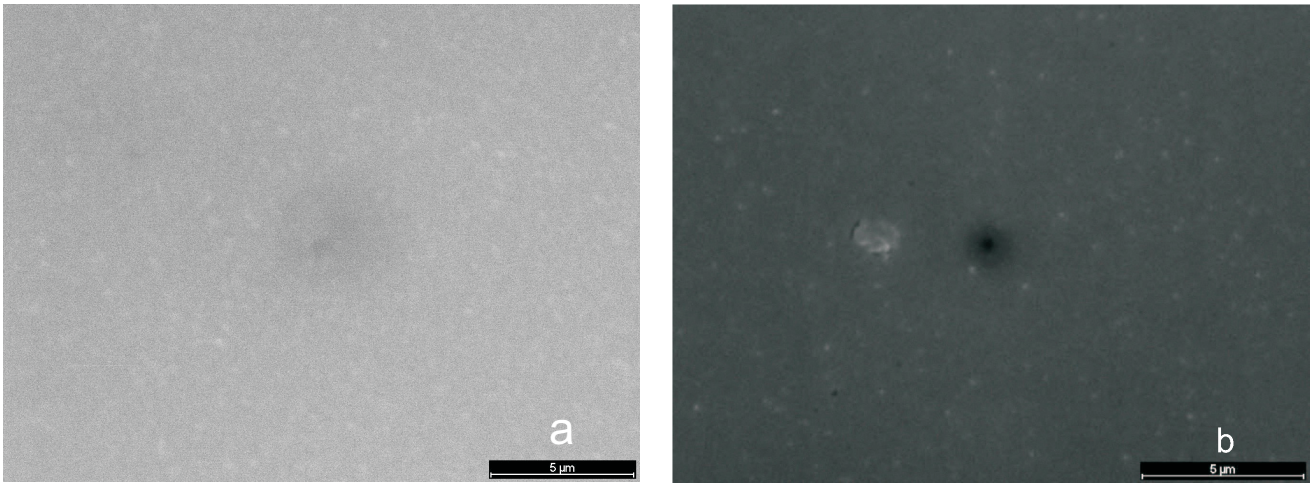

Figure 20. Micrographs of parylene C [(**a**) CVD, the scale bar is 5 µm; (**b**) PECVD, the scale bar is 5 µm], deposited at a pressure of 22 mTorr (3 Pa).

As AFM measurements reveal (Figure 21), at higher pressures (60 mTorr = 8 Pa), the surface roughness depends strongly on the deposition method. For both derivates, the PECVD film is definitely smoother than the CVD film, where this ratio is higher for parylene N. This corresponds to the hydrophobic conduct of the CVD film, as well as the behavior against water with a contact angle of 60°. For parylene C, the difference is not as distinct, which is reflected in the contact angles. According to the Wenzel equation, a rougher surface is connected with poorer wettability (Lotus effect) [44].

Both effects:

- polar groups that terminate the chains at the surface and
- the smoother surfaces of PECVD layers,

cause better wettability against water. The increasing roughness with rising pressure, which is explicitly depicted in Figures 17 and 21c for CVD parylene N, refers to the higher density of monomers in the vapor; this leads to a higher extent of volume polymerization. Consequently, a lower partial pressure of monomers (at the same total pressure) would cause smoother surfaces. This is shown in Figures 22 and 23, where AFM micrographs are shown, which have been obtained from surfaces deposited at three different degrees of solution (with argon). They have been evaluated applying the program GWYDDION (version 2.32). At same partial pressure of the monomer (6 mTorr), the average roughness decreases with increasing dilution, but at the cost of a lower growth rate (Figure 9).

The surface energy of the films of the N-derivate is at the low-pressure limit of the chlorine-derivate. Other groups report contact angles against water of 90°–103° for parylene C [45–49] and 81°–87° for parylene N, resp. [49,50]. Therefore, their windows are very narrow compared to the widths obtained in this study. Over the whole range investigated, the layers behave hydrophobic in character with only slight deviations.

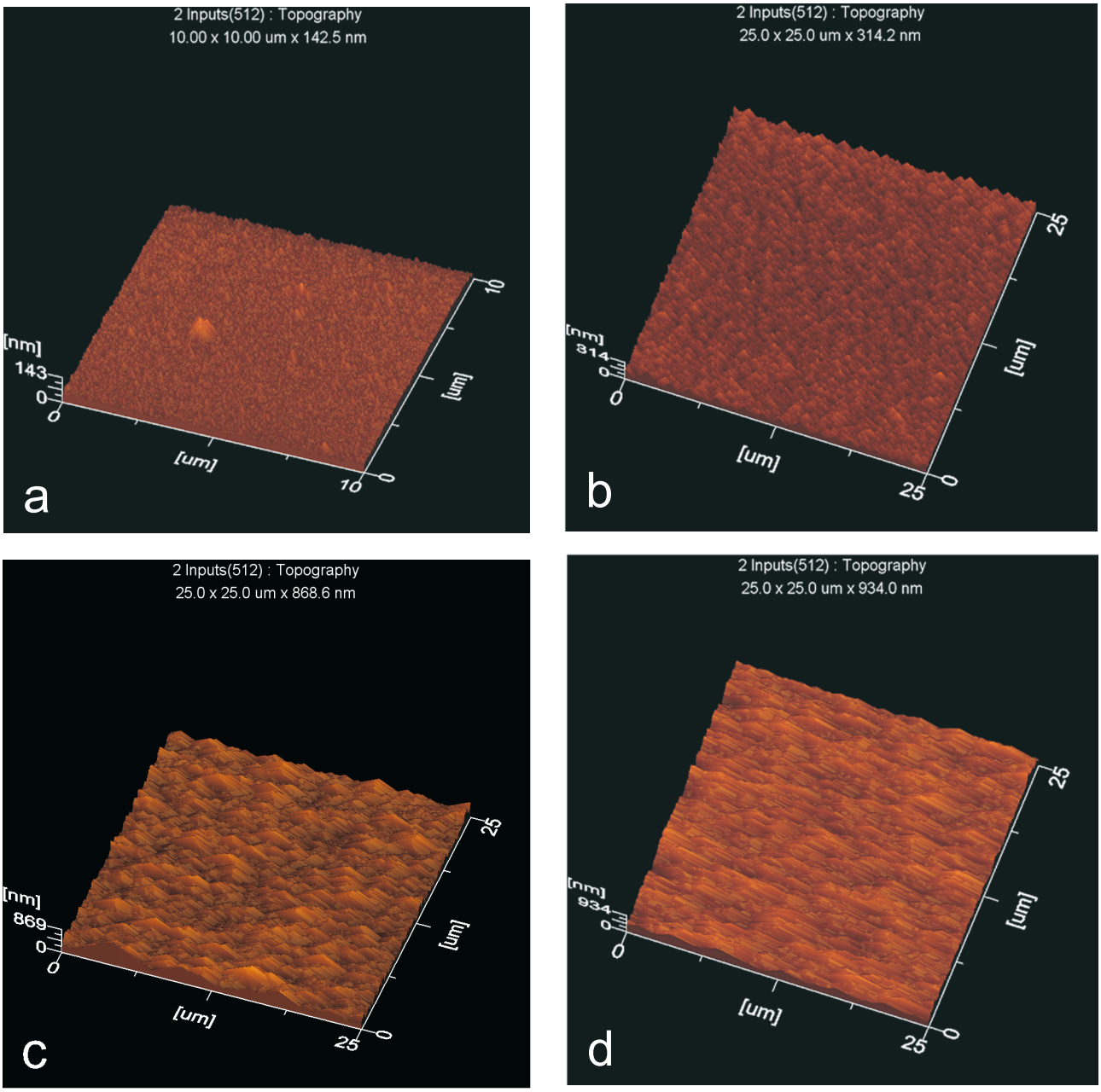

Figure 21. AFM measurements of surfaces smooth and rough in character. Operating pressure: 60 mTorr (8 Pa). (**a**) Parylene N, PECVD; (**b**) parylene C, PECVD; (**c**) parylene N, CVD; (**d**) parylene C, CVD.

3.6.3. Super-Hydrophobic Surfaces

Contact Angle and Surface Energy

The interaction between the surface and a liquid, which causes the phenomenon of wetting, was established by Wenzel [44] and Cassie and Baxter [43]. Following this conception, nanoroughening [6] has become a common technique to generate super-hydrophobic surfaces [51]. In most cases, a multi-step procedure is required. We introduce an easy method by doping the atmosphere with CF_4, which can be applied to PECVD, as well as to CVD. As shown in Figure 24, we covered a flow range

up to more than double the flow of mono-parylene (the flow is 9.1 sccm). Whereas for the CVD layers, the character still remains lipophilic, the plasma-generated film exhibits an opposite conduct with almost an inverted slope. As can be drawn from the evaluation of the surface energy (Figure 25), this is almost completely caused by a large increase of the dispersive fraction in the CVD case, which is opposed by a steep drop in the case of PECVD, whereas the polar fraction remains almost constant in both cases.

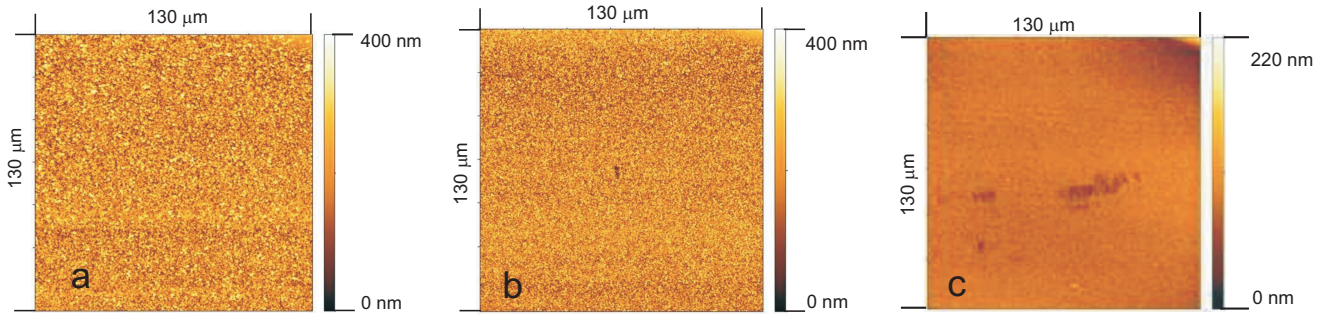

Figure 22. AFM measurements of layers that have been deposited with the same partial pressure of *p*-xylylene, but a different dilution with argon. (**a**) Pure (6 mTorr, 0.8 Pa); (**b**) 37.5 mTorr (5 Pa); (**c**) 75 mTorr (10 Pa).

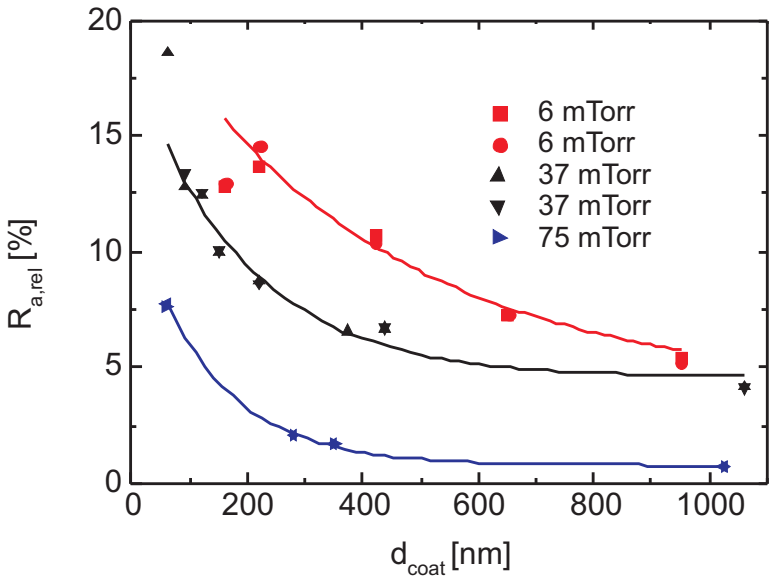

Figure 23. Relative roughness (hole depth ÷ layer thickness as a function of absolute layer thickness) for three different pressures (parylene N). Six millitorrs for the pure ambient gas; the higher pressures are caused by dilution with argon.

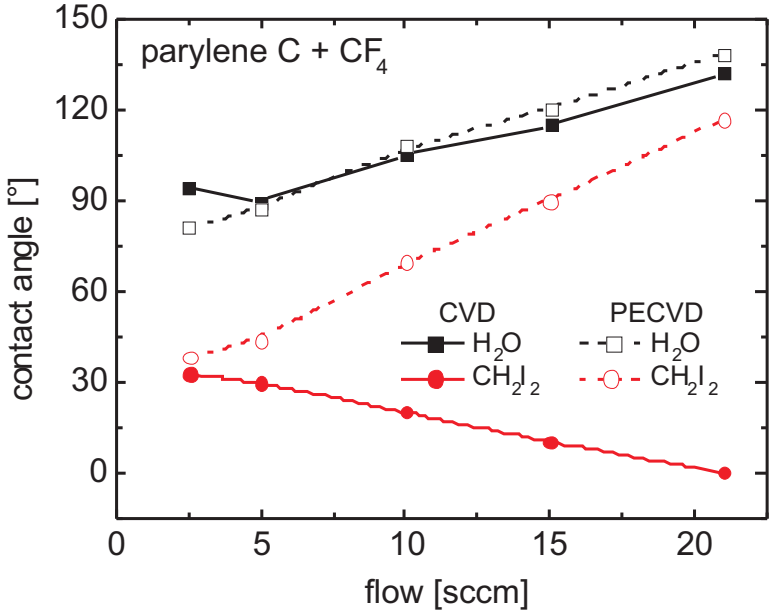

Figure 24. Doping of the atmosphere of parylene C with CF_4 leads to increasing hydrophobic behavior.

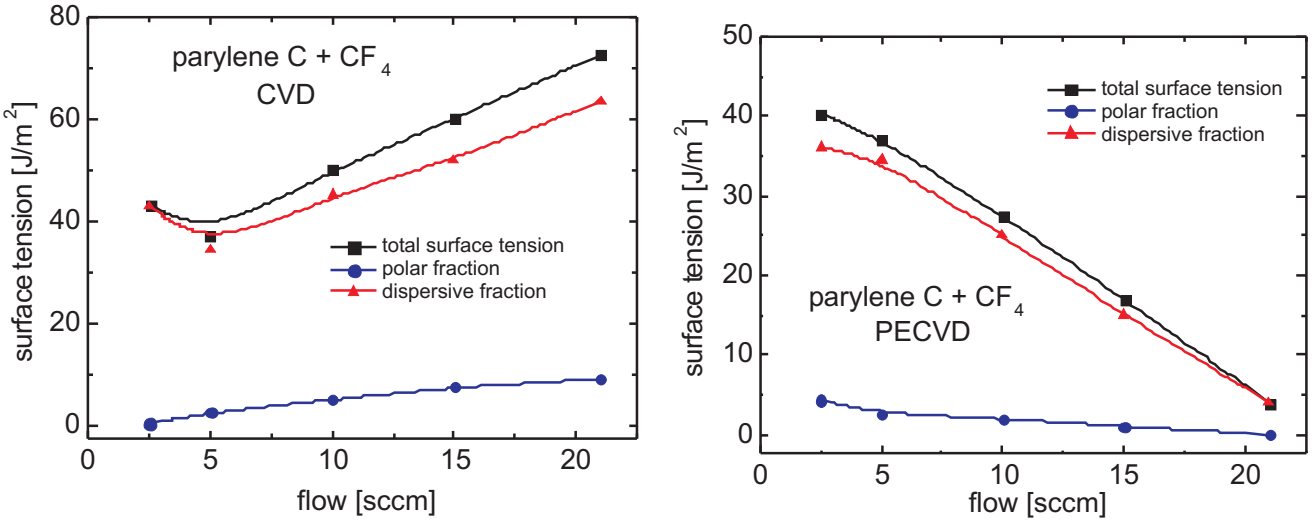

(**a**) (**b**)

Figure 25. Different habits of the surface tension of (**a**) CVD and (**b**) PECVD polyparylene C, doped with CF_4. The microwave power was between 100 and 125 W.

Micrographs (SEM)

This super-hydrophobic behavior has been found to be caused most frequently by a surface that exhibits a roughness in the nano-range [7,8]. This can refer to two main reasons. At high flow rates of the monomeric species, volume polymerization can favor opaque layers. For high powers, fragmentation dominates polymerization, and this also results in opaque layers. In contrast to this observation, the plasma-deposited layers exhibit a relatively smooth surface, and the super-fluidity cannot be referred to the common Lotus effect (Figure 26).

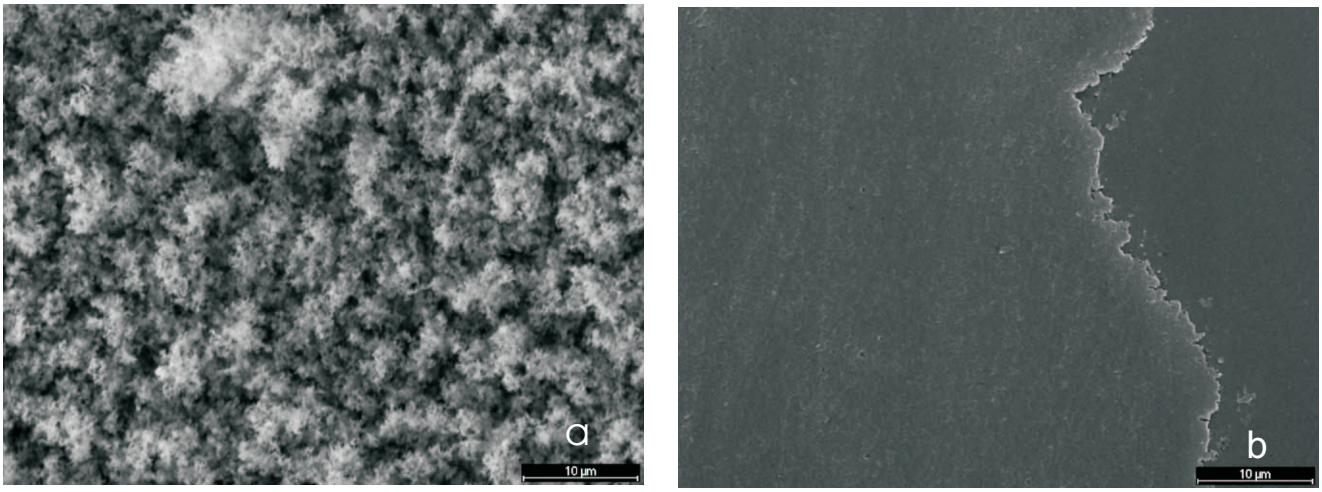

Figure 26. SEM of polyparylene C, copolymerized with CF_4: CVD generates a rough surface at a microscopic scale [(**a**) the scale bar is 10 µm]. Microscopic dust particles in the ambient gas were incorporated during the coating process, resulting in an opaque layer (volume polymerization). PECVD layers maintain their transparency and exhibit a super-hydrophobic performance [(**b**) the scale bar is 10 µm].

The SEM micrographs show the surface with a maximum flow of CF_4, *i.e.*, peaking of the super-hydrophobic effect.

According to the Cassie Equation:

$$\cos\vartheta_{\text{rough}} = rz\cos\vartheta_{\text{smooth}} + (1-z) \tag{4}$$

with ϑ the contact angles for the rough and smooth surfaces (without CF_4 doping), r the surface roughness, z the area fraction of the solid-liquid contact, $1-z$ the area fraction without solid-liquid contact (Cassie or "Fakir" state). We can calculate the border for perfect wetting by organic liquids (here: CH_2I_2) to be reached at a roughness for $r = 1.17$ for CVD parylene C, perfectly lipophilic (contact angle: 0°). Although the roughness of both of the copolymerized layers is very different, their conduct against water is almost congruent and starts at values around 90°. In the vicinity of $\vartheta_{\text{smooth}} = 90\ °$, the contact angle depends very weakly on the roughness itself and rather on the ratio $\frac{1-z}{z}$; at $\vartheta_{\text{smooth}} = 180\ °$, the contact angle would extremely react upon slight variations of $\vartheta_{\text{smooth}}$. According to the Cassie Equation (4), the final values for the contact angle against water in Figure 24 can be explained for the r, z pairs 2,0.09 and 1.4,0.14 for CVD and PECVD, respectively. For both surfaces, the direct solid-liquid contact is very poor, but even worse in the CVD case.

This behavior resembles the observations made by Bi *et al.* [52], who found a superhydrphbic behavior after exposing parylene C to an SF_6/O_2 plasma. They referred this change to the formation of fluorinated groups, proven by the Auger spectrum without significant alterations of the surface roughness: by exchanging –OH by –F as terminating group, F can interact only with external HO-groups, whereas terminating –OH-groups can interact with external OH-groups, as well as with C=O-groups and other electronegative groups.

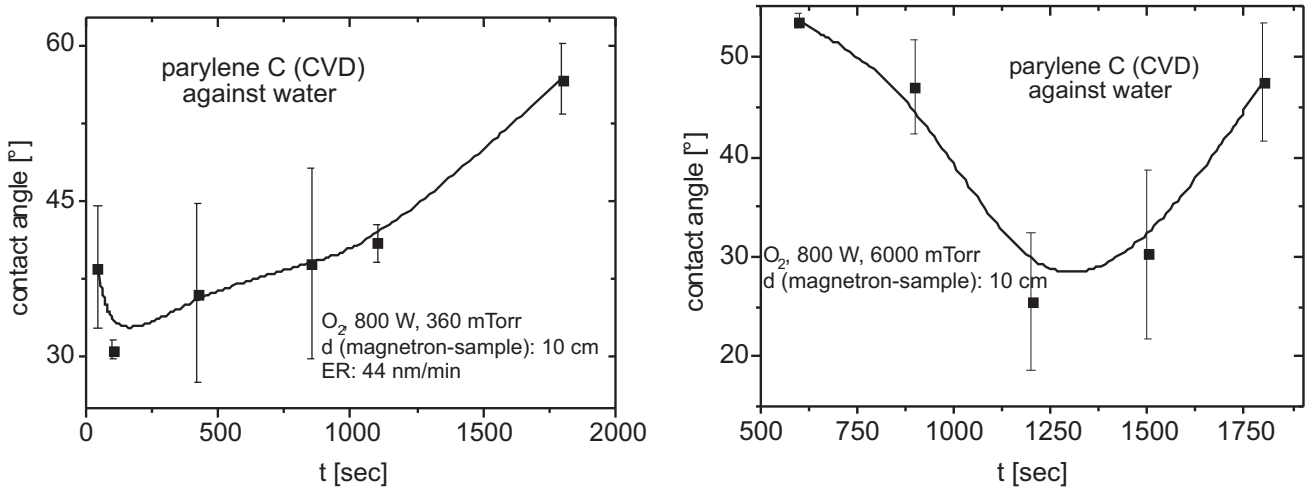

(**a**) (**b**)

Figure 27. Contact angle of parylene C layers deposited with CVD and subsequent oxygen treatment at two different discharge pressures [(**a**) 360 mTorr, 800 W, (**b**) 6000 mTorr, 800 W]. The conduct against water is completely altered. Due to the higher etch rate at 6000 mTorr, the parylene layer is removed entirely after an exposure time of 1300 sec.

3.6.4. Functionalization to Hydrophilic Surfaces

The films deposited from an ambient gas consisting of the pure ambient gas or the pure ambient gas enriched with some CF_4 remain hydrophobic or will turn to super-hydrophobic performance [53]. One method to switch the functionality to hydrophilic behavior can easily be performed by a plasma treatment with oxygen [54]. As shown in Figure 27, where the change of the film quality is depicted as a function of the time of plasma treatment, this surface activation (replacement of hydrophobic C–H bonds by hydrophilic C–OH bonds) leads to contact angles against water down to 30°, but at the expense of layer thickness.

A further increase is correlated with longer times of treatment; eventually, this process leads to the starting values when the layer has been completely etched away. After three weeks of storage, values increase slightly, but the general tendency towards hydrophilicity does not turn back. The rising hydrophilic character refers to the congruent slope of the polar fraction of the surface tension (Figure 28). This conduct has been communicated also by Olson [38], who observed the same phenomenon also for exposing the parylene film to a plasma of the inert gas argon and a retreat of hydrophilicity after about one day. Bi *et al.* report on perfect wetting after exposure to an O_2-RF plasma [52]. Tsougeni *et al.* applied an O_2 plasma to increase the hydrophilicity of polymethacrylates [55]. However, the original value was never reached. The trend to hydrophilicity for PECVD-generated films and this hydrophilization are caused by the same source, namely oxygen; however, in the first case this was unintended.

A second way is the copolymerization with oxygen. As shown in Figure 29, for both of the excitation techniques, a change in surface conduct is feasible. Again, the values for the hydrophilic behavior as measured by the drop pendant method are better (lower) for plasma excitation than for the thermal variant. The values reach flat values almost of 20 °C.

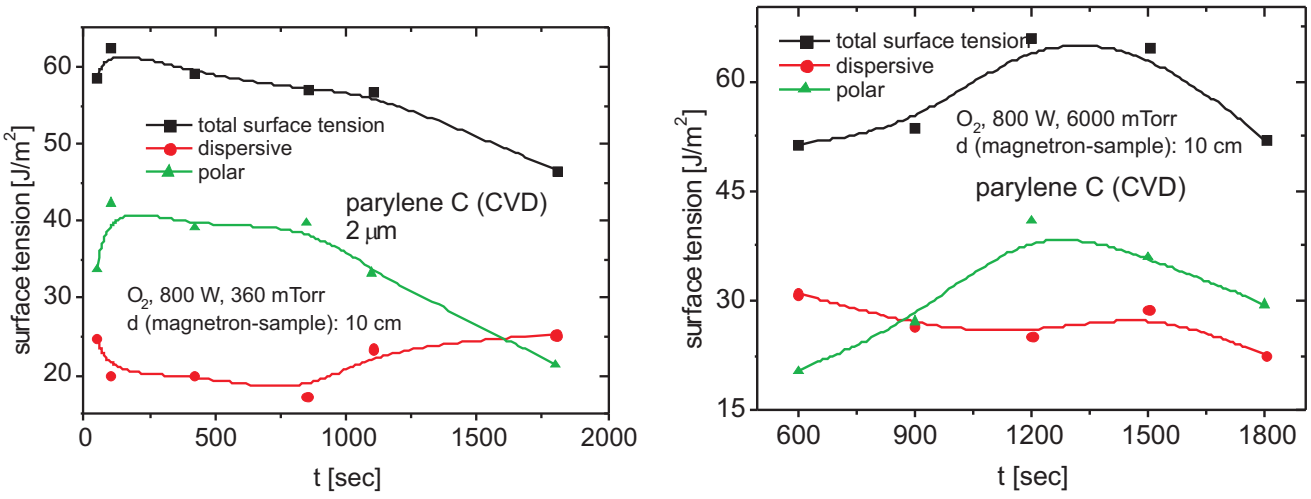

Figure 28. Surface energy of parylene C layers deposited with CVD and subsequent oxygen treatment at two different discharge pressures [(**a**) 360 mTorr, 800 W, (**b**) 6000 mTorr, 800 W]. The conduct against water is completely altered.

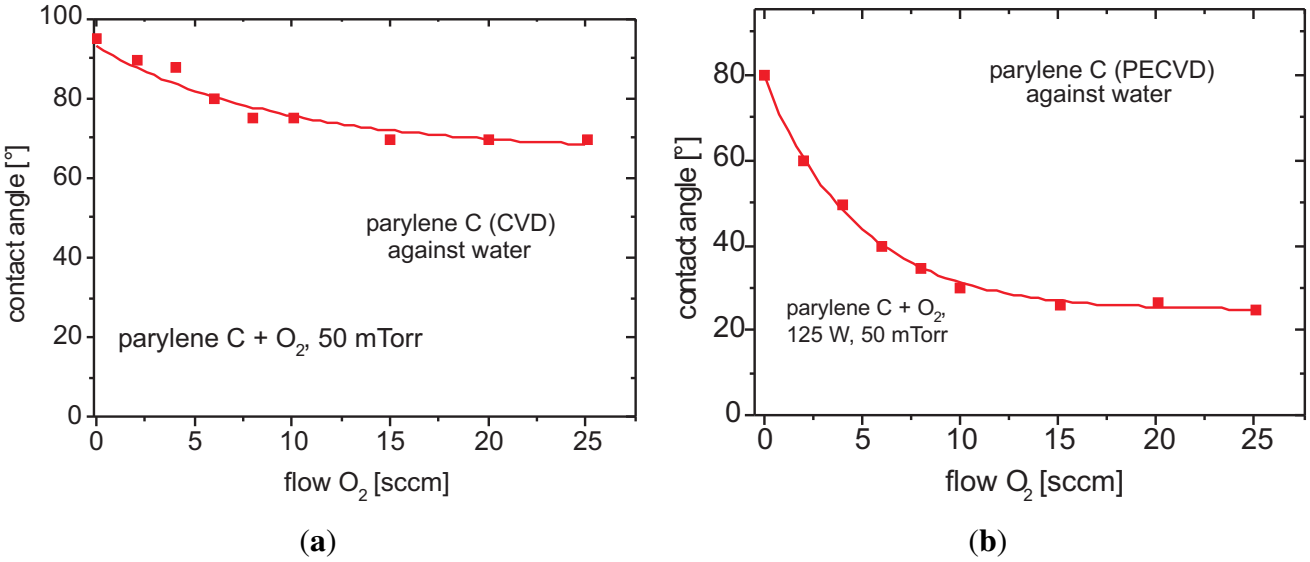

Figure 29. Contact angle of parylene C layers co-deposited with oxygen with (**a**) CVD and (**b**) PECVD. The tendency towards hydrophilicity is obvious.

4. Conclusions

The behavior of parylene films that were deposited with CVD and PECVD has been investigated. We can group these results into two categories, thermally-activated CVD, typically driven at a dissociation temperature of 700 °C, and plasma-activated CVD, typically driven below a microwave power density of 1.5 W/L. The upper limit for the second method is set by the onset of the destruction of the monomers (benzene rings) whose structure elements cannot be detected by IR spectroscopy any more.

The efficiency of polymerization depends on the density of active and functional monomers. Beyond 400 °C, thermal activation generates active monomers. Plasma activation of functional monomers is

limited to about 1.5 W/cm^2. Due to the decline of electron temperature and plasma density with rising pressure, this effect becomes less pronounced with increasing pressure.

The surface quality is very sensitive to changes of the plasma parameters studied, especially the degree of dilution with an inert gas, by which the type of polymerization can be changed from a reaction that mainly happens in the vapor to a reaction that mainly occurs on the surface. Most of the deposits are expected to act hydrophobically, which they actually do, but the surface can be made hydrophilic either by sole plasma monomerization without thermal support where a real coincidence between plasma density and hydrophilic behavior is observed or by a subsequent oxygen treatment. In this case, the film is slowly removed by oxidation. The hydrophilic surface remains stable for at least four weeks. A third path is opened with copolymerization, with oxygen yielding high performance low contact angles against water for both of the excitation methods.

Plasma-assisted copolymerization with CF_4 also changes the nature of the deposit, this time to super-hydrophobic behavior. The surface remains relatively smooth, indicating that the process still remains in the regime of surface polymerization. The same amount of CF_4, added to a CVD process, shifts the process into the regime of volume polymerization, which is evidence by a rough surface.

Acknowledgment

This paper comprises some works of Stanislav Dribinskiy, Florian Schamberger and Astrid Ziegler. Thanks are due to Rosi Heilmann from Technische Universität München, who took the AFM micrographs. Financial support of the federal secretary of education and research under Numbers 1715X04 and 1753X08 is gratefully acknowledged.

Author Contributions

M.-C.A. and G.F. conceived and designed the experiments; A.R. performed the experiments; A.R. and G.F. analyzed the data; the work has been carried out in the Laboratory for Surface Refinement and Thin Film Technology of Munich University of Applied Sciences and in Walter Schottky Institute of Technische Universität München which is directed by M.-C.A.; A.R. and G.F. wrote the paper.

Conflicts of Interest

The authors declare no conflict of interest.

References

1. Fortin, J.B.; Lu, T.-M. *The Growth and Properties of Parylene Thin Films*; Kluver Academic Publishers: Dordrecht, Netherlands, 2004.
2. Odian, G. *Principles of Polymerization,* 4th ed.; Wiley-Interscience: New York, NY, USA, 2004.
3. Zhang, X.; Dabral, S.; Chiang, C.; McDonald, J.F. Crystallinity properties of parylene-N affecting its use as an ILD in submicron integrated circuit technology. *Thin Solid Films* **1995**, *270*, 508–512.
4. Yasuda, H. *Plasma polymerization*; Academic Press Inc.: New York, NY, USA, 1985.

5. Yang, G.R.; Ganguli, S.; Karcz, J.; Gill, W.N.; Lu, T.M. High deposition rate parylene films. *J. Cryst. Growth* **1998**, *183*, 385–390.
6. Franz, G. Plasma roughening of polished SiC substrates. *Mater. Sci. Semicond. Process.* **2003**, *5*, 525–531.
7. Tserepi, A.D.; Vlachopoulou, M.-E.; Gogolides, E. Nanotexturing of poly(dimethylsiloxane) in plasmas for creating robust super-hydrophobic surfaces. *Nanotechnology* **2006**, *17*, 3977–3983.
8. Kokkoris, G.; Constantoudis, V.; Angelikopoulos, P.; Boulousis, G.; Gogolides, E. Dual nanoscale roughness on plasma-etched Si-surfaces: Role of etch inhibitors. *Phys. Rev. B* **2007**, *76*, doi:10.1103/PhysRevB.76.193405.
9. Lu, B; Lin, J.C.-H.; Liu, Z; Lee, Y.-K.; Tai, Y.-C. Highly flexible, transparent and patternable parylene-C superhydrophobic films with high and low adhesion. In Proceedings of 24th International Conference MEMS, Cancun, Mexico, 23–27 January 2011; pp. 1143–1146.
10. Morris, J.R. Electrosurgical instrument having a parylene coating. U.S. Patent 5,380,320 A, 9 November 1993.
11. Vitek Research Corporation. Parylene coating. Availabe online: http://vitekres.com/coatings/parylene-coatings (accessed on 5 May 2015).
12. Hanyaloglu, B.; Aydinli, A.; Oye, M.; Aydil, E.S. Low dielectric constant Parylene-F-like films for intermetal dielectric applications. *Appl. Phys. Lett.* **1999**, *74*, 606–608.
13. Juneja, S.; Ten Eyck, G.A.; Bakruand, H.; Lu, T.-M. Pressure dependent Parylene-N pore sealant penetration in porous low-κ dielectrics. *J. Vac. Sci. Technol. B* **2005**, *23*, 2232–2235.
14. Gorham, W.F. A new, general synthetic method for preparation of linear poly-pxylylenes. *J. Polym. Sci. A* **1966**, *4*, 3027–3039.
15. Demirel, M.C.; Cetinkaya, M.; Singh, A.; Dressick, W. A Non-covalent method for depositing nanoporous metals via spatially organized poly(p-xylylene) films. *Adv. Mater.* **2007**, *19*, 4495–4499.
16. Cetinkaya, M. *Synthesis and Characterization of Nanostructured Poly-(p-xylylene) Films*. Ph.D. Thesis, Pennsylvania State University, Pittsburgh, PA, USA, 2008.
17. Stahl, U. Entwicklung eines Verfahrens zur Stabilisierung von Polymerschichten auf OFW-Sensoren für die Analytik von organischen Gasen. Ph.D. Thesis, Techn. University of Karlsruhe, Karlsruhe, Germany, 1999.
18. Lin, T.J.; Chun, B.H.; Yasuda, H.K.; Yang, D.J.; Antonelli, J.A. Plasma polymerized organosilanes as interfacial modifiers in polymer-metal systems. *J. Adhes. Sci. Technol.* **1991**, *5*, 893–901.
19. Ishaque, M. Poly(p-xylylene): Synthesen, Strukturen, Eigenschaften und spezielle Anwendungsgebiete. Ph.D. Thesis, Philipps-Universität, Marburg/Lahn, Germany, 1999.
20. Yasuda, H.; Chun, B.H.; Cho, D.L.; Lin, T.J.; Yang, D.J.; Antonelli, J.A. Interface-engineered parylene C coating for corrosion protection of cold-rolled steel. *Corrosion* **1996**, *52*, 169–176.
21. Ganguli, S.; Agrawal, H.; Wang, B.; McDonald, J.F.; Lu, T-M.; Yang, G.-R.; Gill, W.N. Improved growth and thermal stability of parylene films. *J. Vac. Sci. Technol. A* **1997**, *15*, 3138–3142.
22. Franz, G.; Schamberger, F.; Voss, D. Druckgesteuerte Abscheiderate. German Patent Disclosure DE 2012 014 915.8, 29 July 2012.

23. Franz, G.; Schamberger, F. Evaporation and thermal cracking of dimeric parylenes. *J. Vac. Sci. Technol. A* **2013**, *31*, 061602:1–061602:8.
24. Kammer, S.; Wien, S.; Koch, K.P.; Robitzki, A.; Stieglitz, T. Untersuchungen zur Abscheidung von Parylen C als Kapselungsmaterial für biomedizinische Mikroimplantate — Coating material of parylene C as encapsulation material for biomedical micro-implants. *Biomedizin. Technol.* **2002**, *47*, 823–830.
25. Greiner, A.; Mang, S.; Schäfer, O.; Simon, P. Poly(1,4-xylylene)s: Synthesis, polymer analogeous reactions, and perspectives on structure-property relationsships. *Acta Polym.* **1997**, *48*, 1–15.
26. Simon, P.; Mang, S.; Hasenhindl, A.; Gronski, W.; Greiner, A. Poly(1,4-xylylene) and its derivatives by chemical vapor deposition: Synthesis, mechanism, and structure. *Macromolecules* **1998**, *31*, 8775–8780.
27. Ishaque, M.; Agrarwal, S., Greiner, A. Synthesis and properties of novel poly(p-xylylene)s with aliphatic substituents. *e-Polymers* **2002**, *31*, 442–451.
28. Falbe, J.; Regitz, M. *Römpp Chemie Lexikon*; Georg Thieme Verlag: Stuttgart, Germany, 1995.
29. Gerhartz, W.; Elvers, B. *Ullmanns Enzyklopädie der technischen Chemie **15***, 4th ed.; Verlag Chemie: Weinheim/Bergstraße, Germany, 1992; p. 432.
30. Franz, G.; Rauter, F.; Dribinskiy, S.F. Characterization of microwave plasmas for deposition of polyparylene. *J. Vac. Sci. Technol. A* **2009**, *27*, 1035–1041.
31. Schamberger, F.; Ziegler, A.; Franz, G. Influence of film thickness and chemical vapor deposition rate on surface quality of polyparylene coatings. *J. Vac. Sci. Technol. B* **2012**, *30*, 051801:1–051801:6.
32. Franz, G.; Kelp, A.; Meßerer, P. Analysis of chlorine-containing plasmas applied in III/V semiconductor processing. *J. Vac. Sci. Technol. A* **2000**, *18*, 2053–2061.
33. Franz, G. Comprehensive analysis of capacitively coupled chlorine-containing plasmas. *J. Vac. Sci. Technol. A* **2005**, *23*, 369–387.
34. Kaelble, D.H. *Physical Chemistry of Adhesion*; John Wiley: New York, NY, USA, 1971.
35. Rogojevic, S.; Moore, J.A.; Gill, W.N. Modeling vapor deposition of low-K polymers: Parylene and polynaphtalene. *J. Vac. Sci. Technol. A* **1999**, *17*, 266–274.
36. Blackburn, E.V.; Timmons, C.J. The photocyclisation of stilbene analogues. *Quart. Rev.* **1969**, *23*, 482–503.
37. Beach, W.F. A Model for the Vapor deposition polymerization of *p*-Xylylene. *Macromolecules* **1978**, *11*, 72–76.
38. Olson, R. Xylylene polymers. In *Encyclopedia of Polymer Science and Engineering*, 2nd ed.; Wiley: New York, NY, USA, 1989; Volume 17, pp. 990–1024.
39. Mitu, B.; Bauer-Gogonea, S.; Leonhartsberger, H.; Lindner, M.; Bauer, S.; Dinescu, G. Plasma-deposited parylene-like thin films: process and material properties. *Surf. Coat. Technol.* **2003**, *174–175*, 124–130.
40. Streitwieser, Jr., A.; Ward, H.R. Organic compounds in microwave discharges: II. Initial studies with toluene and related hydrocarbons. *J. Am. Chem. Soc.* **1963**, *85*, 539–542.
41. Wertheimer, M.R.; Moisan, M. Comparison of microwave and lower frequency plasmas for thin film deposition and etching. *J. Vac. Sci. Technol. A* **1985**, *3*, 2643–2649.

42. Moisan, M.; Barbeau, C.; Claude, R.; Ferreira, C.M.; Margot, J.; Paraszczak, J. Sá, A.B.; Sauvé, G.; Wertheimer, M.R. Radio frequency or microwave plasma reactors? Factors determining the optimum frequency of operation. *J. Vac. Sci. Technol. B* **1991**, *9*, 8–25.
43. Cassie, A.B.D.; Baxter, S. Wettability of porous surfaces. *Trans. Faraday Soc.* **1944**, *40*, 546–550.
44. Wenzel, R.N. Resistance of solid surfaces to wetting by water. *Ind. Eng. Chem.* **1936**, *28*, 988–994.
45. Hwang, K.S.; Park, J.H.; Lee, J.H.; Yoon, D.S.; Kim, T.S.; Han, I.; Noh, J.H. Effect of atmospheric-plasma treatment for enhancing adhesion of Au on parylene-C-coated protein chips. *J. Korean Phys. Soc.* **2004**, *44*, 1168–1172.
46. Senkevich, J.J.; Mitchell, C.J.; Vijayaraghavan, A.; Barnat, E.V.; McDonald, J.F. Unique structure/properties of chemical vapor depositied parylene E. *J. Vac. Sci. Technol. A* **2002**, *20*, 1445–1451.
47. Coburn, J.W.; Winters, H.F. Plasma etching—A discussion of mechanisms. *J. Vac. Sci. Technol.* **1979**, *16*, 391–403.
48. Shin, Y.S.; Cho, K.; Lim, S.H.; Chung, S.; Park, S.-J.; Chung, C.; Han, D.-C.; Chang, J.K. Pdms-based micro PRC chip with parylene coating. *J. Micromech. Microeng.* **2003**, *13*, 768–774.
49. Pruden, K.G.; Sinclair, K.; Beaudoin, S. Characterization of parylene-N and parylene-C photooxidation. *J. Polym. Sci. Part A Polym. Chem.* **2003**, *41*, 1486–1496.
50. Zhuang, Y.X.; Menon, A. Wettability and thermal stability of fluorocarbon films deposited by deep reactive ion etching. *J. Vac. Sci. Technol. A* **2005**, *23*, 434–439.
51. Yeo, J.; Choi, M.J.; Kim, D.S. Robust hydrophobic surfaces with various micropillar arrays. *J. Micromec. Microeng.* **2010**, *20*, doi:10.1088/0960-1317/20/2/025028.
52. Bi, X.; Crum, B.P.; Li, W. Super hydrophobic parylene-C produced by consecutive O_2 and SF_6 plasma treatment. *J. Microelectromech. Sys.* **2014**, *23*, 628–635.
53. Liston, E.M.; Martinu, L.; Wertheimer, M.R. Plasma surface modification of polymers for improved adhesion: A critical review. *J. Adhesion Sci. Technol.* **1993**, *7*, 1091–1127.
54. Liston, E.M. Plasma treatment for improved bonding: A review. *J. Adhesion* **1989**, *30*, 199–218.
55. Tsougeni, K.; Petrou, P.S.; Tserepi, A.; Kakabakos, S.E.; Gogolides, E. Nano-texturing of poly(methyl metacrylate) polymer using plasma processes and applications in wetting control and protein absorption. *Microelectron. Eng.* **2009**, *86*, 1424–1427.